Tephrosia purpurea (Linn.) attenuates progression of acute liver failure by reducing oxidative stress and inflammation via modulating cytoprotective enzyme hemoxygenase-1 activity

Samrat Rakshit (samratrakshit007@gmail.com)
Guru Ghasidas Vishwavidyalaya: Guru Ghasidas University https://orcid.org/0000-0001-6283-2847
Nisha Sahu
Guru Ghasidas Vishwavidyalaya: Guru Ghasidas University
Satendra Kumar Nirala
Guru Ghasidas Vishwavidyalaya: Guru Ghasidas University
Shamli S Gupte
Jiwaji University
Sangeeta Shukla
Jiwaji University
Sadhana Shrivastava
Jiwaji University
Bhawana Bhadauria
Department of Ayurvedic and Unani Services
Monika Bhadauria
Guru Ghasidas Vishwavidyalaya: Guru Ghasidas University

Research Article

Keywords: Acute hepatitis, D-Galactosamine, Hemoxygenase-1, HPLC, Inflammation, Lipopolysaccharide, Natural antioxidants, Oxidative stress, Reactive oxygen species, Tephrosia purpurea

Posted Date: May 17th, 2022

DOI: https://doi.org/10.21203/rs.3.rs-1596610/v1

Abstract

Background: Acute liver failure (ALF), often associated with elevated oxidative stress and sustained inflammation, is one of the major clinical manifestations of liver disease with limited therapeutic options. *Tephrosia purpurea* is mentioned in *Ayurvedic* literature to be effective against various health problems. Additionally, this plant with various unknown bioactive components has not been fully explored against acute organ injury, especially against D-galactosamine and lipopolysaccharide induced acute hepatitis. Thus, we aimed to characterize and investigate the efficacy of hydroethanolic extract of *Tephrosia purpurea* to attenuate ALF progression.

Methods: Different doses of *Tephrosia purpurea* extract (50, 100 and 200 mg/kg) were administered orally once a day for 6 days. *In vivo* injury was induced via intraperitoneal injection of D-galactosamine (300 mg/kg) followed by lipopolysaccharide (50 µg/kg). Presence of bioactive compounds, functional groups, nature and size of particles, thermal properties of the extract were determined.

Results: Levels of lipid peroxidation, proinflammatory cytokines were significantly elevated after D-galactosamine and lipopolysaccharide administration that were restored by the administration of *Tephrosia purpurea* via modulating hemoxygenase-1 enzyme. *Tephrosia purpurea* alleviated serum transaminase levels, hematological variables and markedly reduced histological and ultrastructural alterations. *Tephrosia purpurea* reduced iron overload and maintained glutathione homeostasis (P£ 0.05). Not only that, it also eliminated lipid droplets, restored biomacromolecule homeostasis, maintained stability of the membrane, cellular organelles and the DNA.

Conclusions: These findings provided novel insights into the anti-inflammatory and antioxidative mechanisms of *Tephrosia purpurea* and suggested its use as a potential therapeutic candidate against ALF.

Introduction

Acute liver failure (ALF) or acute liver injury (ALI) is one of the severe forms of liver disease. Pathological characteristics include extensive hepatic necrosis with severe loss of parenchyma, violent oxidative stress, and sustained inflammation. Despite enormous clinical efforts, prognosis and high mortality rate haven't improved significantly [1, 2]. Administration of specific hepatotoxin D-galactosamine (D-GalN) in combination with endotoxin lipopolysaccharide (LPS) greatly induces acute liver injury and mimics liver disease in human. This model of acute liver injury is extensively used worldwide to study underlying mechanism of ALF and develop effective therapeutic drugs [1, 2]. It is indispensable that D-GalN and LPS induce oxidative stress and inflammatory responses, which promotes hepatic necrosis, contributing directly in the occurrence and progression of ALF. Therefore, taking care of increased oxidative stress and inflammation may be the first step for the treatment of ALF [3]. Cytoprotective enzymes such as heme oxygenase (HO)-1 play major role in the well-being of a cell under immense oxidative stress and inflammation. Thus, modulation of these cytoprotective enzymes related to oxidative stress and inflammation could be an effective therapeutic strategy for D-GalN and LPS induced ALF [4].

Traditional systems of medicine remain invaluable since ages due to their multiple health outcomes and minimal side effects as compared to modern drugs [5]. These plants have long been thought to be potential hepatoprotective agents for their various biological activities including antioxidant and anti-inflammatory by regulating multiple signal molecules [5]. The use of crude plant extracts as therapeutic supplement showed various plausible health benefits including amelioration of metabolic complications, oxidative stress and inflammation induced injury [6]. Plants possess many advantageous biologically active phytochemicals with minimal to no side effects, when taken as a part of human diet or at effective doses [7]. Phytochemicals present in plant extract often exert synergistic effect in improving the efficacy of plant extracts than administered alone. Thus, various plants are often screened for beneficial effect in ameliorating health problems [8].

Tephrosia purpurea (Linn.) pers. (Fabaceae) is a self-generating tropical perennial herb, known as "Sarwawranvishapaha" in *Ayurveda* for its usefulness in hepatic and splenic disorders, phantom tumor, poisonous bite and almost all type of wounds [9]. The usefulness of *Tephrosia purpurea* is also mentioned in an old *Ayurvedic* literature "Bhavaprakasha Nighantu Guduchyadi Varga, 169" that it can alleviate cough, cure blood related diseases, dyspnea and fever [9, 10]. In modern day, hepatoprotective formulations such as "Tephroli" and "Yakrifit" have *Tephrosia purpurea* as one of their major constituents [11]. *Tephrosia purpurea* is reported to possess multiple phenolic compounds including glycosides, flavonoids and flavones, responsible for its various protective properties [9, 12, 13]. *Tephrosia purpurea* showed a very high therapeutic index as the LD_{50} of its ethanolic extract is 2000 mg/kg in rats [14].

Traditional healers claim that *Tephrosia purpurea* is useful in treating diabetes, rheumatism, asthma, diarrhea, ulcers [15], gonorrhea, bronchitis, impotency and other kidney and heart disorders [16]. These claims about *Tephrosia purpurea*, in our traditional healing system need scientific validation to prove its effectiveness. To the best of our knowledge, no scientific literature is available that explains biophysical properties of *Tephrosia purpurea* and its effectiveness, particularly against D-GalN and LPS induced acute liver injury. Thus, present study was focused to investigate biophysical characteristics of *Tephrosia purpurea* and its therapeutic potential against D-GalN and LPS induced acute liver injury.

Materials And Methods

Preparation of hydroethanolic extract of *Tephrosia purpurea*

The plant was identified as *Tephrosia purpurea* (Linn.) pers. and a Voucher no: GGV/BOT/H/FAB/DKS/210 was obtained at Botany Department, Guru Ghasidas University, Chhattisgarh, India. Whole plant of *Tephrosia purpurea* was collected form Guru Ghasidas University campus and air dried in shade for 3 weeks and pulverized. 15 grams of pulverized sample was extracted by Soxhlet apparatus (worm method) for 30 minutes using 70% (v/v) ethanol in

water. The hydroethanolic extract was concentrated in a rotary evaporator and lyophilized. The yield of the extract (2.9g, 19.33%) was obtained preserved for further use.

Reverse phase-HPLC instrumentation and chromatographic conditions

The isocratic reverse phase HPLC analysis was carried out in a Shimadzu HPLC system (LC-20AD) consisted with double pumps (LC 20-AD), column oven (CTO-20AC), sample injector system (SIL-20ACHT) and a spectrophotometric detector (SPD-20A) with a computer assisted analysis software (Shimadzu LC solution 1.25sp1). The stationary phase used for this analysis was a reverse-phase C18 column (150mm × 4.6 mm, 5 μm) and the mobile phase consisted of aqueous acid solution (0.5 M phosphoric acid) : methanol (50 : 50 v/v) mixture with a stable flow rate of 0.9 mL/min. The mobile phase was filtered through 0.45 µm membrane filter and degassed by ultrasonic bath prior to use. The temperature of the column was maintained at room temperature (25 ± 2ºC). 20 μL of each sample were filtered through a 0.22 µm nylon membrane before injecting into the HPLC system for analysis. The presence of bioactive phytochemicals including tannic acid, ascorbic acid, catechin, gallic acid, caffeic acid, rutin, vanillic acid, morin, malic acid, quercetin and ellagic acid were investigated. Presence of these compounds were confirmed by comparing chromatogram peaks of plant extract with reference standards by comparing their retention time. Stock solutions of 40 ppm for all the standard references and 2000 ppm for plant extract were prepared in mobile phase. The detection wavelength was 280 nm for tannic acid, 265 nm for ascorbic acid, 276 nm for catechin, 220 nm for gallic acid, 324 nm for caffeic acid, 260 nm rutin, 220 nm for vanillic acid, 370 nm for morin, 230 nm for malic acid, 256 nm for quercetin and 368 nm for ellagic acid. The detection wavelength for *Tephrosia purpurea* extract was 269 nm. The absorption spectra were determined by UV-VIS spectroscopy.

UV–Vis spectra analysis

Hydroethanolic (70% ethanol in water) extract of *Tephrosia purpurea* at 1000 ppm concentration was observed by UV–Vis spectroscopy within the ranges between 200 nm and 800 nm to identify phytoconstituents containing σ-bonds, π-bonds and lone pair of electrons, chromophores and aromatic rings present in it.

Particle size analysis (PSA)

The crude plant extract, having various particle size ranges were determined using particle size analyzer (Shimadzu's SALD- 2300). Sample was dissolved in 20 ml 70% ethanol followed by sonication for 10 minutes. Particle sizes were measured based on the time dependent scattering of laser light by the particles with a pump speed of 5.0 cm^3/min.

Thermogravimetry analysis (TGA)

The changes in mass of *Tephrosia purpurea* extract over the time with changes in temperature were assessed. Dynamic thermogravimetric curves of extract were obtained by thermogravimetric analysis with Shimadzu's TGA -50, with 10°C/min heating rate ranging from 25°C to a temperature of 800°C under nitrogen atmosphere with a flow of 100 mL/min. The plant extract was packed in a platinum crucible and subjected to analysis. Calcium oxalate monohydrate was used for calibration of the instrument to characterize weight loss steps.

Differential scanning colorimetry (DSC)

The DSC curves of *Tephrosia purpurea* were obtained using a Shimadzu calorimeter, model Shimadzu's DSC-60 Plus. The instrument was coupled to a photovisual system and an oven with a temperature range of 20-300°C. The whole analysis was done under nitrogen atmosphere with constant flow of 100 ml/min and a heating rate of 5°C/min. The plant extract was packed in alumina crucible for analysis.

X-ray diffraction (XRD)

The structural analysis of *Tephrosia purpurea* extract was carried out by using X ray diffraction techniques on Rigaku's Mini Flex 600 diffractometer. The *Tephrosia purpurea* extract was subjected to Cu-Kα radiations (λ=0.154056 nm, 2θ= 2-90°) operating at a voltage of 40 kV and a current of 15 mA, at 10°C/min speed at a drive axis of 2θ. The average size of the crystallite (D in nm) was also calculated from the XRD peak using Debye Scherrer's relation [17, 18].

$$D_{hkl} = \frac{k\lambda}{\beta cos\theta}$$

Where, *k*= 0.9 is the Scherrer's constant**, λ=** 1.540562Å is wavelength of X-rays and β (in radian) is the full width of half maxima (FWHM) of the diffraction peak at an angle θ.

Fourier transform infrared spectroscopy (FT-IR)

Functional groups are responsible for medicinal properties of plants. The whole plant extract of *Tephrosia purpurea* was subject to FT-IR analysis on a Perkin Elmer's Spectrum Two using KBr stressed disks within a spectral range of 4000–450 cm^{-1} to determine presence of possible functional groups.

Experimental animals

Experimental animals (*Wistar* rats, 150±10g) were purchased from Defense Research and Development Establishment, Gwalior, and kept in departmental animal house for 15 days to get acclimatized. Animals were exposed to a 12 h periodic light and dark cycle with a constant temperature about 25°±2°C.

Rats were provided with palleted rat diet and water *ad libitum*.

Animal right

Animal care and experimental procedures were carried out by sincerely following the guidelines set by the committee for the purpose of control and supervision of experiments on animal, India. The experimental procedure was approved by institutional animal ethics committee (994/Ere/Go/06/CPCSEA) on 01/08/2016 (Ref:162/IAEC/Pharmacy/2016).

Chemicals

Pure and analytical grade chemicals were procured from Sisco Research Laboratories Pvt. Ltd (SRL) and Himedia Laboratories Pvt. Ltd., India in this study. LPS (Lot # 114M4009V) was procured from Sigma Aldrich Co Ltd, USA whereas D-GalN (Batch # 3647503) was procured from SRL, India.

D-GalN and LPS model of acute multiorgan injury

The D-GalN and LPS was prepared in saline (0.9% NaCl in water). Acute organ injury was induced by D-GalN (300 mg/2ml/kg) and LPS (50µg/2ml/kg) administered intraperitonially as per previous scientific literature [19].

Preparation of different doses of *Tephrosia purpurea* extract

Freeze dried plant extract was dissolved in distilled water using 1% (w/v) gum acacia as the suspending agent [19]. Three different doses of *Tephrosia purpurea* (50 mg/kg, 100 mg/kg and 200 mg/kg) were taken for evaluation where the highest dose (200 mg/kg) corresponds to $1/10^{th}$ of the LD_{50}.

Experimental design

Well acclimatized thirty-six animals were divided equally into six groups. Group I: designated as control, received 1% gum acacia as vehicle. Group II: designated as TP *per* se, received 200 mg/kg dose of *Tephrosia purpurea* extract. Group III: designated as D-GalN+LPS (experimental control), received 300 mg/kg dose of D-GalN followed by 50 µg/kg dose of LPS. Group IV-VI: designated as TP50, TP100 and TP200 respectively, received 50, 100 and 200 mg/kg dose of *Tephrosia purpurea* extract respectively along with D-GalN and LPS. Vehicle and different doses of *Tephrosia purpurea* were given orally for 6 days straight to their respective groups. The D-GalN followed by LPS (only after 1 hour of D-GalN) were given intraperitonially to group III to VI on the 6^{th} day evening. All the animals were fasted overnight and sacrificed 16 hours after D-GalN and LPS treatment using diethyl ether. To generate an individual data point in each of the independent experiments, samples were used in triplicates.

Hematological study

Blood was collected by puncturing retro-orbital venous sinus into heparinized tubes and kept at 4°C for hematological studies. Analysis of blood for determining white blood cell count (WBC), red blood cell count (RBC), platelet count (PLT), hemoglobulin (Hb), hematocrit (HCT), lymphocyte and monocyte count was done by semi-automatic blood analyzer (Analytica HEMA 2062+) [20].

Serological study

The blood was also collected in heparin free tubes and allowed to clot at room temperature for 30 minutes. The blood was centrifuged to obtain serum for determination of serological parameters such as aspartate aminotransferase (AST), alanine aminotransferase (ALT), alkaline phosphatase (ALP), bilirubin, urea, uric acid, creatinine, glucose, triglyceride and cholesterol with the help of respective diagnostic kits following direction of use given on kit manual (The ERBA Chem 5 v 3 Germany).

Oxidative stress assessment in hepatic and renal tissue samples

For determination of lipid peroxidation (LPO), 10% homogenates of hepatic and renal tissues were prepared in KCl solution. The LPO in liver, kidney and microsomes were determined from quantified TBARS [21].

Antioxidant status assessment in hepatic and renal tissue samples

Sucrose solution (1%) was used to prepare homogenates to assess reduced glutathione (GSH) [22]. NaCl (0.9%) was used to prepare tissue homogenates to determine superoxide dismutase [23] and catalase activities [24].

Lipid status in hepato-renal tissue samples

To determine triglycerides [25] and cholesterol [26] in tissue, homogenates of liver and kidney were prepared in chilled hypotonic solution.

Microsomal CYP2E1 activity, protein and lipid peroxidation

Microsomes were prepared by $CaCl_2$ precipitation method [27]. The CYP2E1 activity was determined in terms of aniline hydroxylase activity using aniline as a substrate [28]. Microsomal protein was assessed using Folin and Ciocalteu phenol reagent [29].

Histopathological preparation of hepatic and renal tissue samples

Small pieces of liver and kidney were immediately fixed in Bouin's fixative. Fixed tissues were further processed and embedded in paraffin wax before cutting 05 mm thick sections. Sections were placed on a glass slide and stained with hematoxylin and eosin (H&E) stain [30]. Approximately 10-15 observations for each slide were taken with light microscope.

From the above-mentioned results, it can be clearly observed that, 200 mg/kg dose of *Tephrosia purpurea* perform better than the other two lower doses. Thus, only 200 mg/kg dose of *Tephrosia purpurea* treated groups was further considered for determination of antioxidant enzymes of GSH cycle, proinflammatory cytokines, electron microscopy, genotoxicity and vital parameters of RBC degradation cycle.

Enzymes of GSH cycle in hepato-renal tissue samples

Glutathione reductase [31], glutathione peroxidase [32], glucose-6-phosphate dehydrogenase [33] and glutathione-S-transferase [34] were determined from tissue homogenate freshly prepared in 1.15% KCl solution.

Assessment of proinflammatory cytokines in serum

Proinflammatory cytokines including tumor necrosis factor- α (TNF-α) and interleukin-6 (IL-6) were assessed in serum using ELISA kits (Ray Biotech, Inc; Norcross, GA 30092 USA) to assess inflammation.

RBC degradation cycle in hepatic tissue sample

Hepatic hemoglobin [35], heme content [36], ferritin [37], hemosiderin [38], iron [39], bilirubin [40], biliverdin [41], biliverdin reductase [42] and hemoxygenase-1 (HO-1) enzyme [43], were determined in freshly prepared liver homogenate.

Processing of hepatic and renal tissue samples for ultra-structural observation

Liver and kidney tissue of about 1 mm^3 in size were fixed immediately in Karnovsky's fixative and then in 1% osmium tetroxide [44]. Fixed tissues were eventually embedded in resin and were cut into 70-90 nm thick sections and placed on a copper grid. The grid along with tissue sections were stained with positive staining (Uranyl acetate and lead citrate) prior to the observation with transmission electron microscope [45, 46].

Genotoxicity study in hepato-renal tissue samples

Single cell gel electrophoresis study was performed to observe genotoxicity [47]. Liver tissue homogenate (10%) was taken on a thin film of agarose spread glass slide. Slides were placed in electrophoresis buffer to start electrophoresis. Slides were immediately washed with HCl buffer and stained with ethidium bromide to observe with a microscope. Images were analyzed by ImageJ software.

Statistical analysis

Results are expressed as mean ± SE (n=6). Data were analyzed for statistical significance using one-way analysis of variance ($P \leq 0.05$) followed by Tukey's *post hoc* honestly significant difference test (*post hoc* HSD test) to draw a comparison among different treatment groups ($P \leq 0.05$) [48] using Microsoft Excel worksheet-2019. A p value ≤ 0.05 was considered as significant.

Results

HPLC fingerprinting analysis of *Tephrosia purpurea* extract

The HPLC fingerprinting analysis of *Tephrosia purpurea* extract and other standards are summarized in Fig 1. *Tephrosia purpurea* extract showed various phytochemicals as evident by presence of peaks at various retention time. Based on the retention time, compounds were identified and presented in table 1. Results revealed the presence of some medicinally active well-known phytoconstituents as well as some unknown compounds. The first peak between retention time 2 to 4 comprises multiple active components including tannic acid (2.806), L-ascorbic acid (2.964), catechin (2.920), gallic acid (3.269) and caffeic acid (3.639). The peak at 4.020 is rutin (4.035), peak at 4.542 is vanillic acid (4.517), peak at 5.442 is morin (5.447) or malic acid (5.489), peak at 6.260 is quercetin (6.379) and the peak at 7.349 is ellagic acid (7.265). There were some unidentified peaks at retention time 9.581, 12.026, 18.342 and 23.398.

UV-Vis Spectral analysis of *Tephrosia purpurea* extract

Scanning analysis of the extract showed two peaks at UV range as well as one in visible range. The peaks at 260, 280 and 660 nm showed absorption of 3.994, 3.721, 0.242 respectively (Fig. 2). The first peak appeared at 260 nm was intense than that of 280 nm. A very light peak appeared at 660 nm suggested presence of colored compound in the extract.

Particle size analysis of *Tephrosia purpurea* extract

Fig. 3 represents the histograms of the dispersed particles present in *Tephrosia purpurea* extract as obtained from particle size analyzer. The size of the particles ranges between 0.031 to 0.071 µm. The percentile of particle size of particular diameter was explained in table 2. The most common particle size was 44 nm which comprises of 24.24%. The average particle size of 43 nm was determined from the mean value of the histograms.

TGA and DSC analysis of *Tephrosia purpurea* extract

The thermogram from TGA analysis of *Tephrosia purpurea* extract (Fig. 4A) showed thermal decomposition processes, which occurs between 126.58°C and 266.80°C with a midpoint at 241.33°C. The total weight loss was 17.188 mg (62.001%).

The DSC curves of *Tephrosia purpurea* extract (Fig. 4B) showed thermal reaction processes, which occur between 18.64 and 128.49°C. The event of endothermic reaction was observed at 21.46 (D = 15.56 J g^{-1}) and 120.88°C (D = 32.24 J g^{-1}). Several other endothermic and exothermic peaks were observed between 128.49 and 232.28°C. The major weight loss was observed between 200-500°C.

X-ray powder diffraction analysis of *Tephrosia purpurea* extract

The diffractogram obtained from XRPD analysis of *Tephrosia purpurea* hydroethanolic extract showed 10 sharp peaks of variable height at various 2θ (theta) values (Fig. 5). XRD pattern showed presence of crystals in the extract. The crystallite size was calculated using the XRD data, suggested the presence of nanoparticles in the size range between 25 nm and 47 nm. The average crystallite size of the plant extract was found to be 34.3 nm.

Furrier transform infrared spectroscopy of *Tephrosia purpurea* extract

The FT-IR spectra of *Tephrosia purpurea* extract (Fig. 6) showed absorbance bands centered at 523, 1044, 1178, 1285, 1403, 1587, 2849, 2917 and 3216 cm^{-1}. Different band Peak represented different functional group present in the extract (Table 3).

Effect of *Tephrosia purpurea* extract on hematological variables

Table 4 represents alterations in different hematological variables after combined administration of D-GalN and LPS. Total number of RBCs, platelets, amount of hemoglobin in blood and hematocrit value were significantly declined, whereas differential cell counting of WBCs, including lymphocytes and monocytes were significantly raised (P£0.05). Treatment of *Tephrosia purpurea* showed dose dependent protection in most of the hematological variables. The 50 mg/kg dose of *Tephrosia purpurea* significantly checked monocytes count towards control. The 100 mg/kg dose boosted hemoglobin, RBCs, hematocrit in one hand and on the other hand, controlled WBCs, including monocytes significantly. The 200 mg/kg dose of *Tephrosia purpurea* significantly protected all the studied variables from alteration. It was observed that the 100 and 200 mg/kg doses of *Tephrosia purpurea* exhibited considerably therapeutic effects in comparison to 50 mg/kg dose.

Effect of *Tephrosia purpurea* extract on serological variables and hepatic glycogen

Table 5 exemplifies protective effect of *Tephrosia purpurea* pretreatment against toxic demonstration of D-GalN and LPS on serological variables. Exposure to D-GalN and LPS resulted in substantial increase of serum transaminases (AST and ALT), ALP, urea, uric acid and creatinine (P£0.05). All the three doses of *Tephrosia purpurea* provided protection against toxic outcome of D-GalN and LPS on serological indices. The 100 and 200 mg /kg dose of *Tephrosia purpurea* offered better protection in comparison to 50 mg/kg dose.

Administration of D-GalN and LPS caused considerable upsurge of serum triglyceride, cholesterol and bilirubin, whereas level of albumin, glucose and hepatic glycogen were dwindled abruptly (Table 6). All the three doses of *Tephrosia purpurea* instigated reduction in triglycerides, cholesterol and bilirubin while increment in albumin, glucose and hepatic glycogen was noted towards their respective control. The 100 mg/kg dose was better than 50 mg/kg in reducing triglycerides and bilirubin level. The 200 mg/kg dose of *Tephrosia purpurea* appeared as better protective force in all the parameters except triglyceride and cholesterol in serum. It was also revealed that 200 mg/kg dose was better than 100 mg/kg dose in maintaining bilirubin and triglycerides.

Effect of *Tephrosia purpurea* extract on oxidative stress

The LPO was found to be enhanced drastically in hepatic and renal tissues (Fig. 7) after D-GalN and LPS intoxication (P£0.05). Pretreatment of *Tephrosia purpurea* at all the three doses repressed hepatorenal LPO towards control (P£0.05). *Tephrosia purpurea* at 100 and 200 mg/kg dose was more effective than 50 mg/kg dose in decreasing LPO in both tissues. Dose of 200 mg/kg was more efficient than 100 mg/kg in reducing LPO.

Effect of *Tephrosia purpurea* extract on antioxidant status

The GSH was significantly demoted (Fig. 7) in hepatorenal tissues after D-GalN and LPS exposure (P£0.05). Administration of *Tephrosia purpurea* increased GSH level in all the tissues at 50 mg/kg dose. Tukey's *post hoc* analysis disclosed the fact that *Tephrosia purpurea* at all doses showed similar recovery pattern in uplifting tissue GSH level. The 100 mg/kg dose of *Tephrosia purpurea* showed no significant disparity with control when hepatic GSH was considered only. The 200 mg/kg dose of *Tephrosia purpurea* has no such difference with control even the renal GSH was considered too.

Enzymatic activity of superoxide dismutase and catalase (Fig. 7) in hepatic and renal tissues was severely declined (P£0.05) after exposure to D-GalN and LPS. In *Tephrosia purpurea* treated groups, activity of superoxide dismutase and catalase was found to be enhanced in dose dependent manner. The 100 mg/kg dose of *Tephrosia purpurea* was better than 50 mg/kg dose in recovering enzymatic activity of hepatic superoxide dismutase and catalase. The 200 mg/kg dose had better protective efficacy in enhancing superoxide dismutase and catalase activities towards their respective control.

Effect of *Tephrosia purpurea* extract on tissue lipid profile

Effect of D-GalN and LPS administration on triglycerides and cholesterol in hepatic and renal tissues (P£0.05) have been summarized in Fig. 8. A sharp rise in triglycerides and cholesterol in hepatic and renal tissues was observed. The 100 mg/kg dose of *Tephrosia purpurea* significantly reversed renal triglycerides and hepatic cholesterol as compared to 50 mg/kg dose. The 50 and 200 mg/kg dose of *Tephrosia purpurea* showed significant differences in recovering hepatorenal triglycerides and cholesterol. The 100 and 200 mg/kg dose showed almost identical recovery pattern. *Tephrosia purpurea* at 200 mg/kg dose treated group reversed the variables very much near to control.

Effect of *Tephrosia purpurea* extract on microsomal LPO, protein and CYP2E1 activity

Acute hepatic injury induction by D-GalN and LPS resulted amplified microsomal LPO and CYP2E1 activity (P£0.05), whereas microsomal protein was severely diminished (Fig. 9). *Tephrosia purpurea* treatment resettled microsomal LPO, protein and CYP2E1 activity towards control. *Tephrosia purpurea* at 100 and 200 mg/kg dose were better when compared to 50 mg/kg dose in maintaining LPO and CYP2E1 activity. *Tephrosia purpurea* showed dose dependent recovery pattern for hepatic CYP2E1 activity. All the altered values were found very near to control in 200 mg/kg dose of *Tephrosia purpurea* treated group.

Histopathological observations

Photomicrographs of hepatic and renal histological observations suggested structural component disorganization in D-GalN and LPS exposed group. Prophylactic treatment with *Tephrosia purpura* at three different doses appreciably protected hepato-renal tissues from these alterations. The hepatic and renal histological observations were explained in legends to figures 10 and 11, respectively. Quantitative representation of variables to assess hepato-renal injury as well as improvement has been presented in table 7 and 8 respectively.

It was observed from above-mentioned variables that, 200 mg/kg dose of *Tephrosia purpurea* extract showed better efficacy than the other two lower doses. Thus, only 200 mg/kg dose of *Tephrosia purpurea* extract treated groups were further considered for the determination of antioxidant enzymes of GSH cycle, electron microscopy, genotoxicity, proinflammatory cytokines (TNF-α and IL-6) and RBC degradation cycle including HO-1.

Effect of *Tephrosia purpurea* extract on enzymes of GSH cycle

Effects of D-GalN and LPS administration on hepatorenal enzymatic antioxidant status (P£0.05) were summarized in Fig. 12. After 16 hours of D-GalN and LPS treatment animals showed significant decrement in glutathione reductase, glutathione peroxidase, glucose-6-phosphate dehydrogenase and glutathione-S-transferase activities was observed in hepatorenal tissue at 5% level of significance. Oral administration of *Tephrosia purpurea* exhibited significant reversal in enzymatic activities of glutathione reductase, glutathione peroxidase, glucose-6-phosphate dehydrogenase and glutathione-S-transferase (*P £ 0.05*) in liver and kidney. *Tephrosia purpurea* showed no substantial difference with control in recovering all these enzymatic antioxidants except for renal glutathione peroxidase.

Effect of *Tephrosia purpurea* extract on proinflammatory cytokines

Administration of D-GalN and LPS significantly induced inflammation via producing proinflammatory cytokines including TNF-α and IL-6 in serum (Fig. 13). The 200 mg/kg dose of *Tephrosia purpurea* extract significantly (P £ 0.05) protected the elevation of these cytokines.

Effect of *Tephrosia purpurea* extract on RBC degradation cycle

Table 9 depicted therapeutic effect of *Tephrosia* on the components of RBC degradation cycle against toxic exposure to LPS and D-GalN. The bilirubin, biliverdin, Hb, heme, free iron (ferritin and hemosiderin) and heme iron along with biliverdin reductase and HO-1 activities in the hepatic tissue were significantly elevated (Table 9) after D-GalN and LPS intoxication (P £ 0.05). *Tephrosia purpurea* at 200 mg/kg dose showed therapeutic effect on all the variables by reducing their level towards control in liver cells except HO-1 activity. The HO-1 activity was further induced up to 3.4 folds by *Tephrosia purpurea* at 5% level of significance as compared to control. The therapy of *Tephrosia purpurea* at 200 mg/kg dose was able to recover most of the variables altered due to inflammation and oxidative stress induced by LPS and D-GalN.

Ultra-structural observations

Electron microscopic study of liver and kidney have been presented in figure 14. The figure of control liver depicted regular hepatocytes with obvious nuclear membrane (NM) with visible nuclear pores (NP), dense cytoplasm, numerous well-formed mitochondrion (M) and rough endoplasmic reticulum (RER) around nuclear membrane (Fig. 14A). The D-GalN and LPS administered rat (Fig. 14B) showed loss of nuclear membrane integrity, dilated endoplasmic reticulum and mitochondrial degeneration. Loss of genetic material as indicated by the electron lucent area inside the nucleus and steatosis indicated by deposition of lipid droplets (LD) were also observed (Fig. 14B).

Prophylactic treatment with *Tephrosia purpurea* extract at 200 mg/kg dose (Fig. 14C) showed almost regular shaped nucleus with well-maintained nuclear membrane and nucleolus. Homogenous distribution of euchromatin throughout the nuclear area, regular shaped and more dense mitochondria were also observed along with fine network of ER attached to the nucleus. Decreased steatosis and more dense cytoplasm were noticed as compared to the D-GalN and LPS exposed group.

Electron micrograph obtained from transmission electron microscopy revealed that control kidney showed its regular architecture with well-defined membranes, mitochondrial abundance and peroxisomes with circular outline and homogenous content (Fig. 14D). The D-GalN and LPS administered rats showed swelling in mitochondria, loss of cytoplasmic and mitochondrial structural integrity, and lipid droplet accumulation in the cytoplasm (Fig. 14E).

Prophylactic treatment with 200 mg/kg dose of *Tephrosia purpurea*showed better mitochondrial structure, reduced lipid droplet accumulation and peroxisome with homogenous content (Fig. 14F).

Effect of *Tephrosia purpurea* extract on genetic material

Exposure to D-GalN and LPS caused severe damage to DNA in hepatorenal tissue. DNA damage was studied in terms of comet assay (Fig. 15) and its numeric data is presented in table 10. Exposure to D-GalN and LPS induced fragmentation of DNA in liver and kidney (Fig. 15, A-F). A significant increase in tail length and high movement translated it into comet and was considered as DNA damage. Comparison between control group (Fig. 15, A and D) and D-GalN + LPS (Fig. 15, B and E) administered group suggested that D-GalN and LPS administration causes significant increase in tail length, tail moment and tail DNA % in hepatorenal tissues (Table 10). Therapy of 200 mg/kg dose of *Tephrosia purpurea* controlled DNA damage significantly as indicated by decreased tail length and tail moment (Fig. 15, C and F).

Discussion

Bioactive phytoconstituents are well-known for their protective roles against a variety of health problems including acute organ injury. As *Tephrosia purpurea* extract have major phytoconstituents including rutin, gallic acid, quercetin and many more, they might be responsible for its protective efficacy in this present study [19]. Furthermore, presence of single or multiple peaks in the UV-Vis spectra is a clear indication of the presence of unsaturated groups and heteroatoms such as Sulphur, Nitrogen and Oxygen. The peak at positions 660 nm indicated presence of organic chromophores [49].

The loss of volatile products in the first step of thermal decomposition below 200°C is mainly due to free water and ethanol, as this event occurs in fusion tracks and with vaporization of the substance [50]. The major weight loss between 200°C and 500°C may be due to the degradation of a wide variety of secondary metabolites, principally phenolics [51].

The FT-IR is the most suitable technique of the non-destructive spectroscopic methods in the analysis of pharmaceutical solids [50]. Since the extract was hydroethanolic, ethanol and water bands could be present in FTIR spectra. The strong absorption band between 3200–3400 cm^{-1} indicated the presence of polymeric hydroxyl derivatives [52]. Carboxylic acids have an absorbance range of 2500–3300 cm^{-1}, thus, bands at 3216, 2917 and 2849 cm^{-1} could be due to OH stretching of carboxylic acids [53]. Carboxylic acid serves as a main pharmaceutical product in curing many health problems, including ulcers, jaundice, stomatitis, fever, wounds, edema and rheumatic joint pains [52]. The more intense bands occurring at 2917 cm^{-1} and 2849 cm^{-1} corresponding to C–H stretching vibrations could also be attributed to the presence of carbonyl functional groups [52] or methylene group of aliphatic compounds [54]. The absence of any peak between 2220 and 2260 cm^{-1} indicated absence of any toxic substances as this region comprises of cyanide groups [52]. A band at 1587 cm^{-1} could be attributed to C = C bonds in the aromatic rings due to presence of flavonoids and amino acids [50, 55]. The bands at 1403 cm^{-1} would be related to C-H bending vibration of methyl group. The band at 1285 cm^{-1} is probably related to C–O stretching of polyols [55]. The band at 1178 cm^{-1} and 1044 cm^{-1} could be related to C–O stretching and –OH deformation of primary and tertiary alcohols respectively [56]. This band could also be related to C–O stretching of ether, esters and carboxylic acids. This indicated the presence of a wide variety of metabolites, such as tannins, flavonoids, carbohydrates (polysaccharides) and anthraquinones among others [57–59]. The band at 523 cm^{-1} indicated the presence of iodate or brominate compounds [54], which plays role of disinfectant [52].

The XRPD analysis of *Tephrosia purpurea* extract exhibits several size dependent features leading to an irregular peak position, height and width. The sharp peak reveals that the extract is crystalline in nature and the particles are in the Nano regime [60]. The remaining peaks may be due to other phytochemicals present in *Tephrosia purpurea* extract [61].

Studies have suggested that D-GalN and LPS induced hepatorenal injury involves many mechanisms, including oxidative stress, inflammation, apoptosis and necrosis [62]. Compromised cellular integrity due to increased LPO, resulted leakage of cellular constituents especially transaminases (AST and ALT), ALP, bilirubin and albumin into serum impairing liver functions [63]. Various blood components such as WBC, RBC, platelets and hemoglobin gets altered due to sepsis, caused by LPS [19, 63]. Recycling of excess purines due to necrosis increased serum urea, uric acid and creatinine, a clear indication of renal injury [64]. Increase in CYP activity could be attributed to p450 functional failure due to increased requirement of D-GalN and LPS biotransformation with a decrease in protein synthesis and accumulation of triglycerides [19]. Recent studies have shown that antioxidant and anti-inflammatory agents can ameliorate inflammatory responses of LPS induced injury [5]. *Tephrosia purpurea* mainly stabilized the membrane [15] to prevent cellular leakage [65] probably due to the presence of flavonoids that influenced hepatic regeneration [66, 67]. Multiple beneficial functional groups present in *Tephrosia purpurea* extract, as evident in FTIR, might play crucial role in regulating hematological variables, liver and kidney functions.

The D-GalN and LPS trigger excessive reactive oxygen species (ROS), leading to serious oxidative insult in liver injury via lipid peroxidation [62]. Antioxidant molecules such as glutathione, SOD and catalase neutralized oxidative stress by quenching free radicals [67]. The SOD eliminated superoxide anions and produced H_2O_2, which was then decomposed by catalase [68]. *Tephrosia purpurea* protects the depletion of these antioxidant molecules by acting as an antioxidant and provided free electron [9, 66]. GPx harvested electron from glutathione and neutralized free radical by giving free electron, whereas, GR harvested electron from NADPH and reduced oxidized glutathione to make it available again for GPx. Thereafter, G6PDH obtained electron from glucose 6 phosphate, simultaneously converting $NADP^+$ into NADPH by giving that electron. Proper regulation of this cycle helped to maintain antioxidant status, but as cellular ROS increased due to D-GalN and LPS, components of this cycle gets depleted in maintaining redox balance [69]. Glutathione-S-transferase enabled conjugation of glutathione with toxic intermediates to remove them successfully out of the system. Depletion of glutathione-S-transferase, glutathione and CYP2E1 resulted as exposure to D-GalN and LPS produced a number of toxic intermediates upon metabolism [70]. *Tephrosia purpurea* act as a modifier of oxidant response which responded against oxidant-mediated generation of oxidative stress [71]. These enzymes related to GSH cycle were

well maintained by *Tephrosia purpurea* as this plant might have the ability to form conjugates with toxic intermediates and scavenge free radicals [72, 73]. The antihyperlipidemic activity of *Tephrosia purpurea* is might be due to presence of saponins and flavonoids. *Tephrosia purpurea* prevented elevation of triglyceride and cholesterol in D-GalN and LPS exposed animal by increasing the lipoprotein lipase and inhibition of HMG Co A reductase activities respectively [74].

When D-GalN and LPS reaches to the liver, massive pro-inflammatory cytokines including interleukin (IL)-6, IL-1β, and tumor necrosis factor-alpha (TNF-α), were released, leading to serious inflammation damage [62]. The anti-inflammatory activity of *Tephrosia purpurea* helps to reduced inflammation associated hepatorenal injury and maintaining cellular integrity [75]. High production of ROS caused DNA fragmentation and denaturation, thereby, morphological and structural appearance of the nucleus had changed [76]. In the comet assay, the size of the comet's tail signifies DNA damage and the amount of DNA fragments that has migrated from the nucleus determined the tail length [77]. *Tephrosia purpurea* might have quenched free radicals from the nucleus and provided stability to the membrane. As the particles present in the extract are nanosized, they might have interacted with DNA to stabilize it [78].

The rapid degradation of RBCs in the liver is associated with enormous oxidative stress and inflammation, resulted in massive production of heme and iron [79]. Unregulated heme contributed towards oxidative injury via ROS generation as the iron from the heme porphyrin ring is rapidly lost and contributes in ferrous state [80]. Furthermore, ferritin and hemosiderin were released as an acute phase protein to store free intracellular iron [81, 82]. This increased iron deposition in liver which lead to tissue damage and dysregulation of function resulted in increased morbidity and mortality [83]. *Tephrosia purpurea* extract reduced iron overload in liver might be due to having good metal chelating ability [84]. The HO-1 is not only involved in normal physiology but also has a role in pathophysiological states [85]. LPS administration induced release of HO-1 in liver from 6–24 hours [4], but excessive oxidative stress and free heme could also induce HO-1 [86]. Induced HO-1 decreased macrophage infiltration, pro-oxidant and proinflammatory transcription factors to reduce oxidative stress and inflammation in order to protect organs during sepsis. Thus, upregulation of HO-1 is linked with decreased injury during endotoxemia [4]. *Tephrosia purpurea* interfere with RBC degradation and manages to induce HO-1 enzyme up to many folds. HO-1 reduced oxidative stress and inflammation by activating various antioxidant genes to employ cyto-protection [62]. This induced activity of HO-1 may influence other NADPH and oxygen-consuming pathways to reduce oxidative stress [87].

Increased conversion of heme into biliverdin and finally into unconjugated bilirubin by biliverdin reductase leads to the depletion of biliverdin reductase and increased biliverdin accumulation in hepatocytes [88]. Glucuronidation of bilirubin is an essential process to produce conjugated bilirubin for excretion. But, the depletion of uridine-diphosphoglucuronic glucuronosyl transferase (UDPGT) due to D-GalN administration resulted accumulation of unconjugated bilirubin [88, 89]. Administration of *Tephrosia purpurea* might have smoothen the conversion of bilirubin from biliverdin by acting as an alternative of NADPH and glucuronidation of bilirubin by reducing depletion of UDPGT to minimize the accumulation [90, 91].

Similar observation was also reported by Sahu et al., [75]. The phytocompounds present in the hydroalcoholic extract of *Tephrosia purpurea* might be responsible for protecting tissue from oxidative stress and inflammation induced injury by neutralizing those free radicals while enhancing the body's defense systems against degenerative diseases [92, 93].

Conclusion

The pharmaceutical industry disposes of valuable tools used for quality control of products of plant origin and raw materials which require attentive characterization. Characterization of *Tephrosia purpurea* provides important information about its stability, composition, nature and others. This information is valuable to insure its quality and, therefore, its safety and efficacy. The exposure to D-GalN and LPS resulted increase in the level of oxidative stress and inflammation, which leads to acute organ injury. Treatment with bioactive component rich extract of *Tephrosia purpurea* demonstrated inhibition of D-GalN and LPS induced inflammatory response and oxidative stress. Preventive effect was supported by regular serological and hematological values, improved histoarchitecture, ultrastructure, comet assay photographs, induced HO-1, improved enzymatic antioxidant status and controlled lipid peroxidation in vital organs. These findings may provide a new insight to understand the molecular mechanism behind the anti-inflammatory and anti-oxidative action of *Tephrosia purpurea*, and may provide a better understanding of its use as a traditional medicine to treat various inflammatory and oxidative stress disorders.

Abbreviations

ALF = Acute liver failure; ALI = Acute liver injury; ALP = Alkaline phosphatase; ALT = Alanine amino transferase; ANOVA = Analysis of variance; AST = Aspartate amino transferase; $CaCl_2$ = Calcium chloride; CAT = Catalase; CYP2E1 = Cytochrome p 450 2E1; D-GalN = D-galactosamine; DSC = Differential scanning colorimetry; FTIR = Fourier transform infrared spectroscopy; G6PDH = Glucose 6 phosphate dehydrogenase; GPx = Glutathione peroxidase; GR = Glutathione reductase; GSH = Reduced glutathione; G-S-T = Glutathione S transferase; H&E = Hematoxylin and eosin; Hb = Hemoglobulin; HCT = Hematocrit; HO-1 = Hemoxygenase-1; HSD = Honestly significant difference; IL-6 = Interleukin 6; KCl = Potassium chloride; LPO = Lipid peroxidation; LPS = Lipopolysaccharide; NaCl = Sodium chloride; PLT = Platelets; PSA = Particle size analysis; RBC = Red blood cell; ROS = Reactive oxygen species; RP-HPLC = Reverse phase high performance liquid chromatography; SE = Standard error; SOD = Superoxide dismutase; TBARS = Thio-barbituric acid reactive substances; TGA = Thermogravimetric analysis; TNF-α = Tumor necrosis factor alpha; TP = *Tephrosia purpurea;* UV-Vis = Ultra violet-visible spectroscopy; WBC = White blood cell; XRPD = X-ray powder diffraction.

Declarations

Acknowledgements

The first author greatly acknowledged electron microscopy division, AIIMS, New Delhi, India for providing facilities to carry out ultrastructural study.

Funding: The first author greatly acknowledged Department of Zoology, Guru Ghasidas Vishwavidyalaya for providing Laboratory facilities and fellowship. Authors are also grateful to UGC, New Delhi [Startup Grant {20-1/2012(BSR)/20-12(3/2012) (BSR)] for partial financial assistance.

Conflict of interests: There is no conflict of interest between authors for this manuscript. The manuscript is not communicated in any other journal.

Contribution of authors: Samrat Rakshit: Conceptualization, Investigation, Formal analysis, Writing- Original draft preparation. **Nisha Sahu:** Investigation, Formal analysis. **Satendra Kumar Nirala:** Conceptualization, Writing- Review and editing, Supervision, Validation. **Shamli S Gupte:** Formal analysis. **Sangeeta Shukla:** Supervision, Resources. **Sadhana Shrivastava:** Supervision, Validation. **Bhawana Bhadauria:** Validation, Resources. **Monika Bhadauria:** Conceptualization, Writing- Review and editing, Supervision, Validation. All data were generated in-house, and no paper mill was used. All authors agree to be accountable for all aspects of work ensuring integrity and accuracy.

Ethics approval and consent to participate: Not applicable.

Consent for publication: Not applicable.

Availability of data and material: Not applicable.

References

1. Liao CC, Day YJ, Lee HC, Liou JT, Chou AH, Liu FC. ERK Signaling Pathway Plays a Key Role in Baicalin Protection Against Acetaminophen-Induced Liver Injury. Am J Chin Med. 2017;45(1):105–21. doi:10.1142/s0192415x17500082.
2. Tacke F. Targeting hepatic macrophages to treat liver diseases. J Hepatol. 2017;66(6):1300–12. doi:10.1016/j.jhep.2017.02.026.
3. Ansari MA, Raish M, Bin Jardan YA, Ahmad A, Shahid M, Ahmad SF, et al. Sinapic acid ameliorates D-galactosamine/lipopolysaccharide-induced fulminant hepatitis in rats: Role of nuclear factor erythroid-related factor 2/heme oxygenase-1 pathways. World J Gastroenterol. 2021;27(7):592–608. doi:10.3748/wjg.v27.i7.592.
4. Hassan HM, Guo H, Yousef BA, Ping-Ping D, Zhang L, Jiang Z. Dexamethasone Pretreatment Alleviates Isoniazid/Lipopolysaccharide Hepatotoxicity: Inhibition of Inflammatory and Oxidative Stress. Front Pharmacol. 2017;8:133. doi:10.3389/fphar.2017.00133.
5. Mokhtari-Zaer A, Norouzi F, Askari VR, Khazdair MR, Roshan NM, Boskabady M, et al. The protective effect of Nigella sativa extract on lung inflammation and oxidative stress induced by lipopolysaccharide in rats. J Ethnopharmacol. 2020;253:112653. doi:10.1016/j.jep.2020.112653.
6. Leitzmann C. Characteristics. Health Benefits of Phytochemicals. Complement Med Res. 2016;23(2):69–74. doi:10.1159/000444063.
7. Hollman PCH, Katan MB. Absorption, metabolism and health effects of dietary flavonoids in man. Biomed Pharmacother. 1997;51(8):305–10. doi:https://doi.org/10.1016/S0753-3322(97)88045-6.
8. Ziqubu K, Dludla PV, Joubert E, Muller CJF, Louw J, Tiano L, et al. Isoorientin: A dietary flavone with the potential to ameliorate diverse metabolic complications. Pharmacol Res. 2020;158:104867. doi:https://doi.org/10.1016/j.phrs.2020.104867.
9. Khatri A, Garg A, Agrawal SS. Evaluation of hepatoprotective activity of aerial parts of Tephrosia purpurea L. and stem bark of Tecomella undulata. J Ethnopharmacol. 2009;122(1):1–5. doi:10.1016/j.jep.2008.10.043.
10. Palbag S, Dey BK, Singh NK. Ethnopharmacology, phytochemistry and pharmacology of Tephrosia purpurea. Chin J Nat Med. 2014;12(1):1–7. doi:10.1016/s1875-5364(14)60001-7.
11. Negi N, Kalia AN, Brar S, Gauttam VK. Therapeutic potential of Tephrosia purpurea. J Chem Pharm Res. 2015;7(2):574–80.
12. Touqeer S, Saeed MA, Ajaib M. A review on the phytochemistry and pharmacology of genus Tephrosia. Phytopharmacology. 2013;4(3):598–637.
13. Chen Y, Yan T, Gao C, Cao W, Huang R. Natural products from the genus tephrosia. Molecules. 2014;19(2):1432–58. doi:10.3390/molecules19021432.
14. Hussain T, Fareed S, Siddiqui H, Vijaykumar M, Rao CV. Acute and subacute oral toxicity evaluation of Tephrosia purpurea extract in rodents. Asian Pac J Trop Dis. 2012;2(2):129–32.
15. Sandhya S, Venkata KR, Vinod K, Rsnakk C. Assessment of in vitro antacid activity of different root extracts of Tephrosia purpurea (L) Pers by modified artificial stomach model. Asian Pac J Trop Biomed. 2012;2(3):1487-S92.
16. Pandey MM, Khatoon S, Rastogi S, Rawat AK. Determination of flavonoids, polyphenols and antioxidant activity of Tephrosia purpurea: a seasonal study. J Integr Med. 2016;14(6):447–55. doi:10.1016/s2095-4964(16)60276-5.
17. Cullity BD. Elements of X-ray Diffraction. Addison-Wesley Publishing; 1956.
18. Klug HP, Alexander LE. X-ray diffraction procedures: for polycrystalline and amorphous materials. 1974.
19. Rakshit S, Nirala SK, Bhadauria M. Gallic Acid Protects from Acute Multiorgan Injury Induced by Lipopolysaccharide and D-galactosamine. Curr Pharm Biotechnol. 2020;21(14):1489–504. doi:10.2174/1389201021666200615165732.
20. Rakshit S, Shukla P, Verma A, Kumar Nirala S, Bhadauria M. Protective role of rutin against combined exposure to lipopolysaccharide and D-galactosamine-induced dysfunctions in liver, kidney, and brain: Hematological, biochemical, and histological evidences. J Food Biochem. 2021;45(2):e13605. doi:https://doi.org/10.1111/jfbc.13605.

21. Sharma SK, Krishna Murti CR. Production of lipid peroxides by brain. J Neurochem. 1968;15(2):147–9. doi:10.1111/j.1471-4159.1968.tb06187.x.
22. Brehe JE, Burch HB. Enzymatic assay for glutathione. Anal Biochem. 1976;74(1):189–97. doi:10.1016/0003-2697(76)90323-7.
23. Misra HP, Fridovich I. The role of superoxide anion in the autoxidation of epinephrine and a simple assay for superoxide dismutase. J Biol Chem. 1972;247(10):3170–5.
24. Aebi H. Catalase in vitro. Methods Enzymol. 1984;105:121–6. doi:10.1016/s0076-6879(84)05016-3.
25. Neri BP, Frings CS. Improved method for determination of triglycerides in serum. Clin Chem. 1973;19(10):1201–2.
26. Zlatkis A, Zak B, Boyle AJ. A new method for the direct determination of serum cholesterol. J Lab Clin Med. 1953;41(3):486–92.
27. Schenkman JB, Cinti DL. Preparation of microsomes with calcium. Methods Enzymol. 1978;52:83–9. doi:10.1016/s0076-6879(78)52008-9.
28. Kato R, Gillette JR. Effect of starvation on NADPH-dependent enzymes in liver microsomes of male and female rats. J Pharmacol Exp Ther. 1965;150(2):279–84.
29. Lowry OH, Rosebrough NJ, Farr AL, Randall RJ. Protein measurement with the Folin phenol reagent. J Biol Chem. 1951;193(1):265–75.
30. Suvarna KS, Layton C, Bancroft JD. Bancroft's theory and practice of histological techniques E-Book. Elsevier Health Sciences; 2018.
31. Tayarani I, Cloëz I, Clément M, Bourre JM. Antioxidant enzymes and related trace elements in aging brain capillaries and choroid plexus. J Neurochem. 1989;53(3):817–24. doi:10.1111/j.1471-4159.1989.tb11778.x.
32. Paglia DE, Valentine WN. Studies on the quantitative and qualitative characterization of erythrocyte glutathione peroxidase. J Lab Clin Med. 1967;70(1):158–69.
33. Askar MA, Sumathy K, Baquer NZ. Regulation and properties of purified glucose-6-phosphate dehydrogenase from rat brain. Indian J Biochem Biophys. 1996;33(6):512–8.
34. Habig WH, Pabst MJ, Jakoby WB. Glutathione S-transferases. The first enzymatic step in mercapturic acid formation. J Biol Chem. 1974;249(22):7130–9.
35. Flink EB, Watson CJ. A method for the quantitative determination of hemoglobin and related heme pigments in feces, urine, and blood plasma. J Biol Chem. 1942;146(1):171–8.
36. Sinclair PR, Gorman N, Jacobs JM. Measurement of heme concentration. Curr Protoc Toxicol. 2001. doi:10.1002/0471140856.tx0803s00. ;Chap. 8:Unit 8.3.
37. Gabrio BW, Shoden A, Finch CA. Quantitative fractionation of tissue ferritin and hemosiderin. J Biol Chem. 1953;204(2):815–21.
38. Drysdale JW, Ramsay WN. The separation of ferritin and hemosiderin for studies in the metabolism of iron. Biochem J. 1965;95(1):282–8. doi:10.1042/bj0950282.
39. Ramsay WN. The determination of iron in blood plasma or serum. Biochem J. 1953;53(2):227–31. doi:10.1042/bj0530227.
40. Van Roy FP, Meuwissen JA, De Meuter F, Heirwegh KP. Determination of bilirubin in liver homogenates and serum with diazotized p-iodoaniline. Clin Chim Acta. 1971;31(1):109–18. doi:10.1016/0009-8981(71)90367-6.
41. Makos BK, Youson JH. Tissue levels of bilirubin and biliverdin in the sea lamprey, Petromyzon marinus L., before and after biliary atresia. Comp Biochem Physiol A Comp Physiol. 1988;91(4):701–10. doi:10.1016/0300-9629(88)90953-x.
42. Huang TJ. Detection of biliverdin reductase activity. Curr Protoc Toxicol. 2002;Chap. 9: Unit9.4 . doi: 10.1002/0471140856.tx0904s00.
43. McCoubrey WK Jr. Detection of heme oxygenase 1 and 2 proteins and bilirubin formation. Curr Protoc Toxicol. 2001. doi:10.1002/0471140856.tx0903s00. ;Chap. 9:Unit 9.3.
44. Morris JK. A formaldehyde glutaraldehyde fixative of high osmolality for use in electron microscopy. J Cell Biol. 1965;27:1A–149A.
45. Wisse E, Braet F, Duimel H, Vreuls C, Koek G, Olde Damink SW, et al. Fixation methods for electron microscopy of human and other liver. World J Gastroenterol. 2010;16(23):2851–66. doi:10.3748/wjg.v16.i23.2851.
46. Reynolds ES. The use of lead citrate at high pH as an electron-opaque stain in electron microscopy. J Cell Biol. 1963;17(1):208–12. doi:10.1083/jcb.17.1.208.
47. Singh NP, McCoy MT, Tice RR, Schneider EL. A simple technique for quantitation of low levels of DNA damage in individual cells. Exp Cell Res. 1988;175(1):184–91. doi:10.1016/0014-4827(88)90265-0.
48. Snedecor G, Cochran G. Statistical methods. Affiliated East West Press. Iowa State University press. USA. Published by Oxford and IBN Publishing Co. Kolkata-HS Narute et al; 1994.
49. Jain P, Soni A, Jain P, Bhawsar J. Phytochemical analysis of Mentha spicata plant extract using UV-VIS, FTIR and GC/MS technique. J Chem Pharm Res. 2016;8(2):1–6.
50. Fernandes FH, Santana CP, Santos RL, Correia LP, Conceição MM, Macêdo RO, et al. Thermal characterization of dried extract of medicinal plant by DSC and analytical techniques. J Therm Anal Calorim. 2013;113(2):443–7.
51. Deveoglu O, Cakmakcı E, Taskopru T, Torgan E, Karadag R. Identification by RP-HPLC-DAD, FTIR, TGA and FESEM-EDAX of natural pigments prepared from Datisca cannabina L. Dyes Pigm. 2012;94(3):437–42.
52. Ragavendran P, Sophia D, Arul Raj C, Gopalakrishnan V. Functional group analysis of various extracts of Aerva lanata (L.,) by FTIR spectrum. Pharmacologyonline. 2011;1:358–64.

53. Muruganantham S, Anbalagan G, Ramamurthy N. FT-IR and SEM-EDS comparative analysis of medicinal plants, Eclipta alba Hassk and Eclipta prostrata Linn. Rom J Biophys. 2009;19(4):285–94.
54. Sandhya B, Thomas S, Isabel W, Shenbagarathai R. Ethnomedicinal plants used by the Valaiyan community of Piranmalai hills (reserved forest), Tamilnadu, India.-a pilot study. Afr J Tradit Complement Altern Med. 2006;3(1):101–14.
55. Oliveira RN, Mancini MC, Oliveira FCSd, Passos TM, Quilty B, Thiré RMdSM, et al. FTIR analysis and quantification of phenols and flavonoids of five commercially available plants extracts used in wound healing. Matéria. 2016;21(3):767–79.
56. Vardin H, Tay A, Ozen B, Mauer L. Authentication of pomegranate juice concentrate using FTIR spectroscopy and chemometrics. Food Chem. 2008;108(2):742–8. doi:10.1016/j.foodchem.2007.11.027.
57. Correia LP, Procópio JVV, de Santana CP, Santos AFO, de Medeiros Cavalcante HM, Macêdo RO. Characterization of herbal medicine with different particle sizes using pyrolysis GC/MS, SEM, and thermal techniques. J Therm Anal Calorim. 2013;111(3):1691–8.
58. Skotti E, Kountouri S, Bouchagier P, Tsitsigiannis DI, Polissiou M, Tarantilis PA. FTIR spectroscopic evaluation of changes in the cellular biochemical composition of the phytopathogenic fungus Alternaria alternata induced by extracts of some Greek medicinal and aromatic plants. Spectrochim Acta Pt A: Mol Biomol Spectrosc. 2014;127:463–72. doi:10.1016/j.saa.2014.02.113.
59. Capek P, Hríbalová V, Svandová E, Ebringerová A, Sasinková V, Masarová J. Characterization of immunomodulatory polysaccharides from Salvia officinalis L. Int J Biol Macromol. 2003;33(1–3):113–9. doi:10.1016/s0141-8130(03)00075-8.
60. Mehta B, Chhajlani M, Shrivastava B. Green synthesis of silver nanoparticles and their characterization by XRD. Journal of Physics: conference series: IOP Publishing; 2017. p. 012050.
61. Annamalai A, Christina VL, Sudha D, Kalpana M, Lakshmi PT. Green synthesis, characterization and antimicrobial activity of Au NPs using Euphorbia hirta L. leaf extract. Colloids Surf B Biointerfaces. 2013;108:60–5. doi:10.1016/j.colsurfb.2013.02.012.
62. Lv H, An B, Yu Q, Cao Y, Liu Y, Li S. The hepatoprotective effect of myricetin against lipopolysaccharide and D-galactosamine-induced fulminant hepatitis. Int J Biol Macromol. 2020;155:1092–104. doi:10.1016/j.ijbiomac.2019.11.075.
63. Badamjav R, Sonom D, Wu Y, Zhang Y, Kou J, Yu B, et al. The protective effects of Thalictrum minus L. on lipopolysaccharide-induced acute lung injury. J Ethnopharmacol. 2020;248:112355. doi:10.1016/j.jep.2019.112355.
64. Ansar S, Hamed S, AlGhosoon H, AlSaedan R, Iqbal M. The protective effect of rutin against renal toxicity induced by lead acetate. Toxin Rev. 2016;35(1–2):58–62.
65. Sangeetha B, Krishnakumari S. Ameliorates carbon tetrachloride induced hepatic damage in rats. Int J Pharma Bio Sci. 2010;1(2).
66. Gora RH, Baxla SL, Kerketta P, Patnaik S, Roy BK. Hepatoprotective activity of Tephrosia purpurea against arsenic induced toxicity in rats. Indian J Pharmacol. 2014;46(2):197–200. doi:10.4103/0253-7613.129317.
67. Gora R, Baxla S, Kerketta P, Toppo R, Kumar N, Roy B. Ameliorative potential of Tephrosia purpurea extract against arsenic induced toxicity in wistar rats. Vet World. 2013;6(8).
68. Palanivel MG, Rajkapoor B, Kumar RS, Einstein JW, Kumar EP, Kumar MR, et al. Hepatoprotective and antioxidant effect of Pisonia aculeata L. against CCl4-induced hepatic damage in rats. Sci Pharm. 2008;76(2):203–16.
69. Iwalokun BA, Efedede BU, Alabi-Sofunde JA, Oduala T, Magbagbeola OA, Akinwande AI. Hepatoprotective and antioxidant activities of Vernonia amygdalina on acetaminophen-induced hepatic damage in mice. J Med Food. 2006;9(4):524–30. doi:10.1089/jmf.2006.9.524.
70. Cooper AJ, Pinto JT. Cysteine S-conjugate beta-lyases. Amino Acids. 2006;30(1):1–15. doi:10.1007/s00726-005-0243-4.
71. Dalwadi PP, Patel JL, Patani PV. Tephrosia purpurea Linn (Sharpunkha, Wild Indigo): A review on phytochemistry and pharmacological studies. Ind J Pharma Biol Res. 2014;2(01):108–21.
72. Olayinka ET, Ore A, Ola OS, Adeyemo OA. Ameliorative Effect of Gallic Acid on Cyclophosphamide-Induced Oxidative Injury and Hepatic Dysfunction in Rats. Med Sci. 2015;3(3):78–92. doi:10.3390/medsci3030078.
73. Sun J, Ren DD, Wan JY, Chen C, Chen D, Yang H, et al. Desensitizing Mitochondrial Permeability Transition by ERK-Cyclophilin D Axis Contributes to the Neuroprotective Effect of Gallic Acid against Cerebral Ischemia/Reperfusion Injury. Front Pharmacol. 2017;8:184. doi:10.3389/fphar.2017.00184.
74. Dalwadi PP, Patani PV. Anti hyperlipidemic activity of Tephrosia purpurea plant extracts in poloxomer 407 induced hyperlipidemic rats. Int J Pharmacol Res. 2014;4(4):186–93.
75. Sahu N, Mishra G, Chandra H, Nirala S, Bhadauria M. Propolis modulates cellular biochemistry, antioxidants, cytokine profile, histological and ultra-morphological status against antituberculosis drugs induced hepatic injury. 2018;11(11):609–20. doi: 10.4103/1995-7645.246337.
76. Prahalathan C, Selvakumar E, Varalakshmi P, Kumarasamy P, Saravanan R. Salubrious effects of lipoic acid against adriamycin-induced clastogenesis and apoptosis in Wistar rat bone marrow cells. Toxicology. 2006;222(3):225–32. doi:10.1016/j.tox.2006.02.015.
77. Lu Y, Liu Y, Yang C. Evaluating In Vitro DNA Damage Using Comet Assay. J Vis Exp. 2017(128). doi: 10.3791/56450.
78. Edenharder R, Tang X. Inhibition of the mutagenicity of 2-nitrofluorene, 3-nitrofluoranthene and 1-nitropyrene by flavonoids, coumarins, quinones and other phenolic compounds. Food Chem Toxicol. 1997;35(3–4):357–72. doi:10.1016/s0278-6915(97)00125-7.
79. Bian X, Liu X, Liu J, Zhao Y, Li H, Zhang L, et al. Hepatoprotective effect of chiisanoside from Acanthopanax sessiliflorus against LPS/D-GalN-induced acute liver injury by inhibiting NF-κB and activating Nrf2/HO-1 signaling pathways. J Sci Food Agric. 2019;99(7):3283–90. doi:10.1002/jsfa.9541.
80. Wegiel B, Otterbein LE. Go green: the anti-inflammatory effects of biliverdin reductase. Front Pharmacol. 2012;3:47. doi:10.3389/fphar.2012.00047.
81. Adams PC, Barton JC. A diagnostic approach to hyperferritinemia with a non-elevated transferrin saturation. J Hepatol. 2011;55(2):453–8. doi:10.1016/j.jhep.2011.02.010.

82. Koperdanova M, Cullis JO. Interpreting raised serum ferritin levels. BMJ (Clinical research ed). 2015;351:h3692. doi:10.1136/bmj.h3692.
83. Anderson ER, Shah YM. Iron homeostasis in the liver. Compre Physiol. 2013;3(1):315–30. doi:10.1002/cphy.c120016.
84. Ganz T, Nemeth E. The hepcidin-ferroportin system as a therapeutic target in anemias and iron overload disorders. Hematol Am Soc Hematol Educ Program. 2011;2011:538–42. doi:10.1182/asheducation-2011.1.538.
85. Chau LY. Heme oxygenase-1: emerging target of cancer therapy. J Biomed Sci. 2015;22(1):22. doi:10.1186/s12929-015-0128-0.
86. Zhu Y, Luo S, Sabo Y, Wang C, Tong L, Goff SP. Heme Oxygenase 2 Binds Myristate to Regulate Retrovirus Assembly and TLR4 Signaling. Cell Host Microbe. 2017;21(2):220–30. doi:10.1016/j.chom.2017.01.002.
87. Weigel KJ, Lynch SG, LeVine SM. Iron chelation and multiple sclerosis. ASN neuro. 2014;6(1):e00136. doi:10.1042/an20130037.
88. Sedlak TW, Saleh M, Higginson DS, Paul BD, Juluri KR, Snyder SH. Bilirubin and glutathione have complementary antioxidant and cytoprotective roles. Proc Natl Acad Sci U S A. 2009;106(13):5171–6. doi:10.1073/pnas.0813132106.
89. Kutty RK, Maines MD. Purification and characterization of biliverdin reductase from rat liver. J Biol Chem. 1981;256(8):3956–62.
90. Kapitulnik J, Maines MD. Pleiotropic functions of biliverdin reductase: cellular signaling and generation of cytoprotective and cytotoxic bilirubin. Trends Pharmacol Sci. 2009;30(3):129–37. doi:10.1016/j.tips.2008.12.003.
91. Tudor C, Lerner-Marmarosh N, Engelborghs Y, Gibbs PE, Maines MD. Biliverdin reductase is a transporter of haem into the nucleus and is essential for regulation of HO-1 gene expression by haematin. Biochem J. 2008;413(3):405–16. doi:10.1042/bj20080018.
92. Selvan AT, Shaik R, Suthakaran R, Kumar GM. Gastroprotective Activity of Tephrosia Purpurea. Int J Res Ayurveda Pharm. 2013;4(5):759–63. doi:10.7897/2277-4343.04527.
93. Shah R, Kathad H, Sheth R, Sheth N. In vitro antioxidant activity of roots of Tephrosia purpurea Linn. Int J Pharm Pharma Sci. 2010;2(3):30–3.

Tables

Table 1: Multiple bioactive constituents are present in the hydroethanolic extract of *Tephrosia purpurea*

Peak #	Retention time	Phytoconstituents	Area	Hight	Area %	Hight %
1	2-4	Tannic acid, L-ascorbic acid, catechin, gallic acid and caffeic acid	Not measured	Not measured	Not measured	Not measured
2	4.020	Rutin	50067	2964	1.048	2.765
3	4.542	Vanillic acid	181386	11854	3.796	11.058
4	5.442	Morin and malic acid	14559	903	0.305	0.842
5	6.260	Quercetin	508192	11930	10.635	11.129
6	7.349	Ellagic acid	55092	7091	1.153	6.615
7	9.581	Unknown	809107	23292	16.933	21.728
8	12.026	Unknown	342990	5229	7.178	4.878
9	18.342	Unknown	1864374	31651	39.017	29.525
10	23398	Unknown	952551	12287	19.935	11.462

There can be many phytoconstituents present between retention time 2 to 4, so, we did not measured the area and height of the peak.

Table 2: Particle size distribution statistics analysis of *Tephrosia purpurea* extract

Cum Q3 (%)	100.000	99.834	94.601	76.789	54.075	29.834	20.360	0.039
Diff q3(%)	0.166	5.232	17.813	22.713	24.242	9.474	7.525	0.035
Particle diameter (µm)	0.071	0.063	0.056	0.050	0.044	1.949	1.949	0.031
Median Diameter (µm)	0.043							
Modal Diameter (µm)	0.039							
Mean Value (µm)	0.043							
Standard Deviation	0.079							
Refractive Index	1.70-0.20i							

Median: The size of particle where the cumulative line crosses the 50th percentile; Modal: The size of particle that is most often seen; Mean Value: The average size of the particles; Standard Deviation: The amount of variance, in microns, between each trial; Cum Q3 (%) = Cumulative %: The percent of particles below that micron size; Diff q3 (%) = Differential Distribution: The percent of particles at that micron size.

Table 3: Structural analysis of *Tephrosia purpurea* extract by FTIR spectrum

Wave numbers (cm^{-1})	Vibration	Assignment
3216 cm^{-1}	OH stretching	Polymeric hydroxyl derivatives and carboxylic acids
2849 and 2917 cm^{-1}	OH stretching C-H stretching	Carboxylic acid Carbonyl functional groups Methylene group of aliphatic compounds
1587 cm^{-1}	C=C stretching	Aromatic rings of flavonoids and amino acids
1403 cm^{-1}	C–H bending	Methyl group
1285 cm^{-1}	C–O stretching	polyols
1178 cm^{-1}	C–O stretching	Primary alcohol, ether, ester and carboxylic acid
1044 cm^{-1}	–OH deformation	Tertiary alcohol
523 cm^{-1}	C–I/Br stretching	Iodide or Bromide

Table 4: Protective effect of *Tephrosia purpurea* on hematological variables against D-GalN and LPS

Parameters	Groups					
	Control	TP *per se* TP 200 mg/kg	D-GalN+LPS	D-GalN+LPS+ TP 50 mg/kg	D-GalN+LPS+ TP 100 mg/kg	D-GalN+LPS+ TP 200 mg/kg
Hemoglobin (g/dl)	15.4±0.71	15.5±0.71	11.4±0.52*	12.6±0.58*	14.1±0.65	14.9±0.69^{Y}
Hematocrit (%)	44.2±2.03	45.1±2.07	31.5±1.45*	39.1±1.8	41.1±1.89^{Y}	43.2±1.98^{Y}
RBC (10^6/mm^3)	7.66±0.35	7.58±0.35	5.75±0.26*	6.75±0.31	7.18±0.33^{Y}	7.42±0.34^{Y}
WBC (10^3/mm^3)	11.9±0.55	11.8±0.54	16.8±0.77*	14.7±0.68*	13.2±0.61^{Y}	12.8±0.59^{Y}
Platelets (10^3/mm^3)	710±32.6	725±33.3	452±20.7*	521±23.9*	594±27.3^{Y}	651±29.8^{Yj}
Lymphocyte Count (10^2/mm^3)	28.1±1.29	29.3±1.34	63.7±2.92*	61.3±2.81*	56.4±2.59*	43.1±1.98^{Y*jF}
Monocyte Count (10^2/mm^3)	6.80±0.31	6.70±0.31	16.2±0.74*	9.7±0.45^{Y*}	9.20±0.42^{Y*}	8.70±0.40^{Y}

Data are expressed as mean ± SE, (n=6). *P≤0.05 versus Control. ^{Y}P≤0.05 versus D-GalN+LPS. ^{j}P≤0.05 versus TP 50 mg/kg. ^{F}P≤0.05 versus TP 100 mg/kg.

Table 5: Protective effect of *Tephrosia purpurea* on hepatic and renal functions against D-GalN and LPS

Parameters	Groups					
	Control	TP *per se* TP 200 mg/kg	D-GalN+LPS	D-GalN+LPS+ TP 50 mg/kg	D-GalN+LPS+ TP 100 mg/kg	D-GalN+LPS+ TP 200 mg/kg
AST (IU/L)	81.3±3.73	74.1±3.40	471±21.6*	295±13.5^{Y*}	201±9.23^{Y*j}	108±4.96^{YjF}
ALT (IU/L)	36.3±1.66	35.4±1.62	172±7.92*	129±5.93^{Y*}	90.4±4.15^{Y*j}	51.6±2.37^{YjF}
ALP (IU/L)	193±8.86	184±8.45	389±17.8*	297±13.7^{*Y}	248±11.4^{*Y}	212±9.75^{Yj}
Urea (mg/dl)	29.1±1.34	28.8±1.32	70.6±3.24*	58.9±2.70^{Y*}	44.1±2.02^{Y*j}	36.0±1.65^{Yj}
Uric Acid (mg/dl)	1.41±0.06	1.31±0.06	5.01±0.23*	3.97±0.18^{Y*}	2.87±0.13^{Y*j}	2.0±0.09^{YjF}
Creatinine (mg/dl)	0.70±0.03	0.65±0.03	2.03±0.09*	1.91±0.09*	1.42±0.07^{Y*j}	1.03±0.05^{*YjF}

Data are expressed as mean ± SE, (n=6). *P≤0.05 versus Control. ^{Y}P≤0.05 versus D-GalN+LPS. ^{j}P≤0.05 versus TP 50 mg/kg. ^{F}P≤0.05 versus TP 100 mg/kg.

Table 6: Protective effect of *Tephrosia purpurea* on serum biochemical variables and hepatic glycogen against D-GalN and LPS

Parameters	Groups					
	Control	TP *per se* TP 200 mg/kg	D-GalN+LPS	D-GalN+LPS+ TP 50 mg/kg	D-GalN+LPS+ TP 100 mg/kg	D-GalN+LPS+ TP 200 mg/kg
Glucose (mg/dl)	121±5.55	114±5.23	$71.3±3.72^{*}$	$89.5±4.11^{*}$	$102±4.68^{Y}$	$110±5.06^{Yj}$
Triglyceride (mg/dl)	32.3±1.48	30.1±1.38	$120±5.49^{*}$	$86.7±3.98^{Y*}$	$65.8±3.02^{Y*j}$	$51.5±2.36^{*YjF}$
Cholesterol (mg/dl)	21.3±0.97	20.5±0.94	$49.7±2.28^{*}$	$37.2±1.71^{Y*}$	$35.1±1.61^{Y*}$	$29.7±1.36^{Y*j}$
Total Bilirubin (mg/dl)	0.39±0.02	0.37±0.02	$0.89±0.04^{*}$	$0.71±0.03^{Y*}$	$0.59±0.03^{Y*j}$	$0.49±0.02^{Yj}$
Direct Bilirubin (mg/dl)	0.1±0.01	0.11±0.01	$0.70±0.03^{*}$	$0.54±0.02^{Y*}$	$0.39±0.01^{Y*j}$	$0.19±0.01^{YjF}$
Albumin (g/dl)	4.61±0.21	4.74±0.22	$2.41±0.11^{*}$	$2.89±0.13^{*}$	$3.51±0.16^{*Y}$	$4.01±0.18^{Yj}$
Glycogen (mg/100g)	3200±146	3185±146	$1345±61.5^{*}$	$2339±107^{Y*}$	$2555±117^{Y*}$	$2736±125^{Y}$

Data are expressed as mean ± SE, (n=6). *P≤0.05 versus Control. ^{Y}P≤0.05 versus D-GalN+LPS. ^{j}P≤0.05 versus TP 50 mg/kg. ^{F}P≤0.05 versus TP 100 mg/kg.

Table 7: Severity of liver injuries in different treatments.

[–] no alterations; [+] mild alterations; [++] moderate alterations; [+++] severe alterations.

Parameters	Groups					
	Control	TP *per se* TP 200 mg/kg	D-GalN+LPS	D-GalN+LPS+ TP 50 mg/kg	D-GalN+LPS+ TP 100 mg/kg	D-GalN+LPS+ TP 200 mg/kg
Necrosis	–	–	+++	++	+	–
Vacuolation	–	–	+++	++	+	–
Distorted hepatic cords	–	–	+++	+	–	–
Inflammatory cell infiltration	–	–	+++	++	+	–
Pyknotic nuclei	–	–	+++	++	+	–
Damaged central vain	–	–	+++	+	–	–

Table 8: Severity of kidney injuries in different treatments.

[–] no alterations; [+] mild alterations; [++] moderate alterations; [+++] severe alterations.

Parameters	Groups					
	Control	TP *per se* TP 200 mg/kg	D-GalN+LPS	D-GalN+LPS+ TP 50 mg/kg	D-GalN+LPS+ TP 100 mg/kg	D-GalN+LPS+ TP 200 mg/kg
Tubular dilatation	–	–	+++	++	+	–
Tubular degeneration	–	–	+++	++	+	–
Tubular vacuolization	–	–	++	++	+	–
Glomerular damage	–	–	+++	+	–	–
Loss of glomerular space	–	–	+++	+	–	–
Distortion of endothelial lining	–	–	+	–	–	–

Table 9: Protective effect of *Tephrosia purpurea* on RBC degradation cycle in liver

Groups	Hb (mg/100g liver)	Heme (µg/g liver)	Ferritin (µg Fe/g liver)	Hemosiderin (µg Fe/g liver)	Free iron (µg Fe/g liver)	Total Iron (µg Fe/g liver)	Bilirubin (µg/100 g liver)	Biliverdin (µg/100 g liver)	Biliverdin reductase (p mol bilirubin /min/mg protein)	HO-1 (p mol bilirubin /h/mg protein)
Control	7.39±0.48	8.48±0.55	39±2.53	20±1.29	140±9.08	199±12.9	477±30.9	182±11.8	3.52±0.23	21.1±1.37
LPS+D-GalN	12.8±0.83*	50.7±3.29*	162±10.5*	83±5.39*	545±35.4*	790±51.3*	865±56.1*	394±25.6*	7.88±0.51*	47.3±3.07*
LPS+D-GalN+ TP 200 mg/kg	8.4±0.55Y	21.3±1.38Y*	52±3.38Y	33±2.14Y*	175±11.4Y	260±16.9Y	546±35.4Y	217±14.1Y	3.92±0.25Y	91.8±5.96Y*

Data are expressed as mean ± SE, (n=6). *P≤0.05 versus Control. YP≤0.05 versus D-GalN+LPS. JP≤0.05 versus TP 50 mg/kg. FP≤0.05 versus TP 100 mg/kg.

Table 10: Protective effect of *Tephrosia purpurea* on hepato-renal comet assay

Groups	Parameter					
	Hepatic			Renal		
	Tail length	Tail movement	Tail DNA (%)	Tail length	Tail movement	Tail DNA (%)
Control	0.1±0.005	0.002±0.0001	10.0±0.50	0.29±0.015	0.001±0.0001	7.00±0.35
LPS+D-GalN	22.0±1.11*	21.4±1.08*	97±4.88*	24.0±1.21*	23.9±1.20*	82.0±4.12*
LPS+D-GalN+ TP 20 mg/kg	16.0±0.81Y*	13.6±0.68Y*	41±2.06Y*	14.0±0.70Y*	13.2±0.66Y*	47.0±2.36Y*

Data are expressed as mean ± SE, (n=6). *P≤0.05 versus Control. YP≤0.05 versus D-GalN+LPS. JP≤0.05 versus TP 50 mg/kg. FP≤0.05 versus TP 100 mg/kg.

Figures

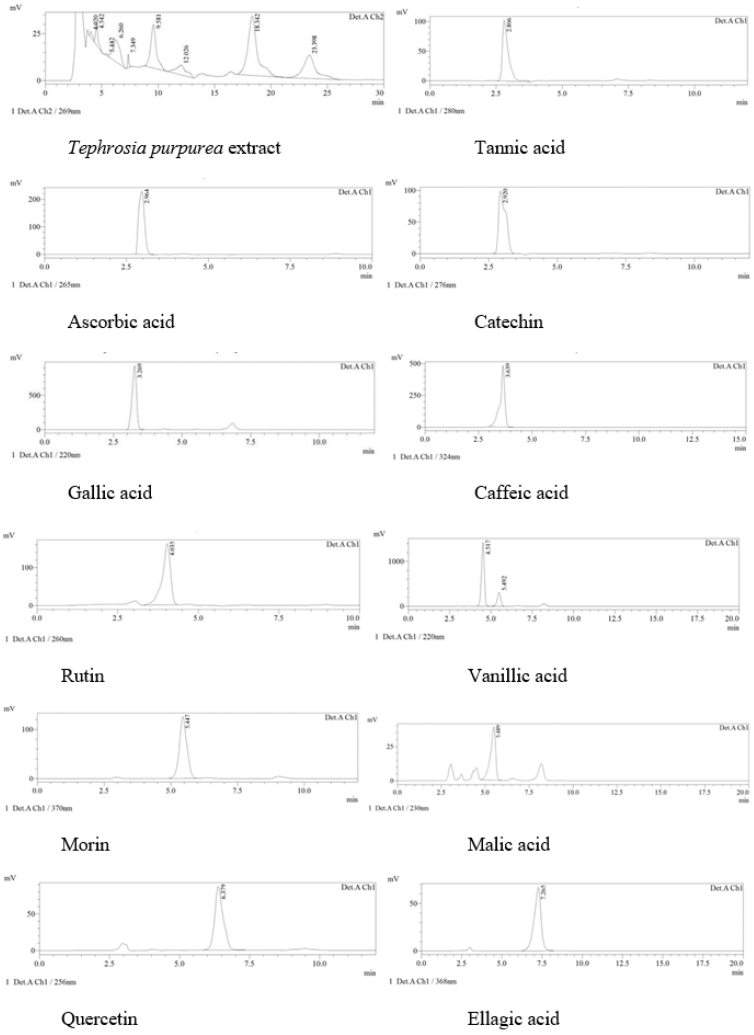

Figure 1

Isocratic HPLC chromatogram of *Tephrosia purpurea* extract and standards obtained under optimum condition

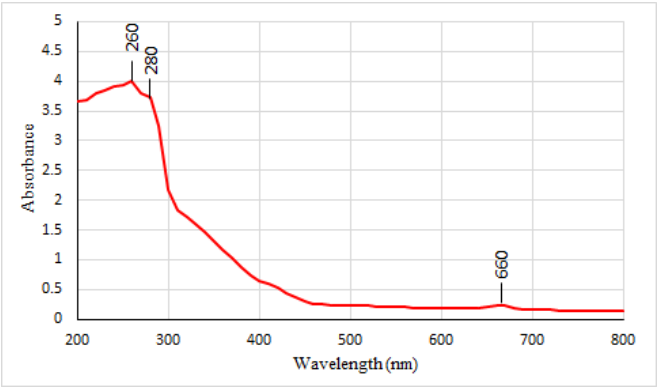

Figure 2

UV-VIS absorption spectra of hydroethanolic extract of *Tephrosia purpurea*

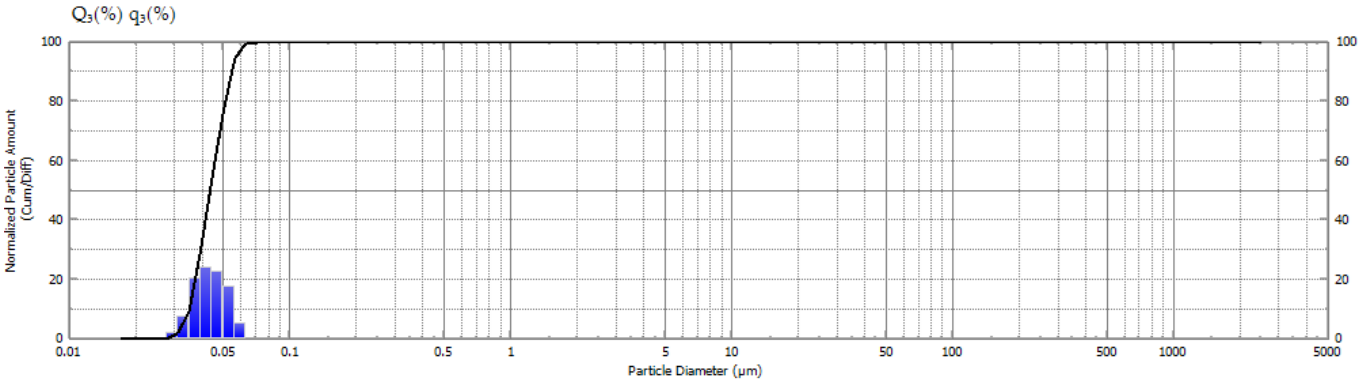

Figure 3

Particle size distribution histogram of hydroethanolic extract of *Tephrosia purpurea*

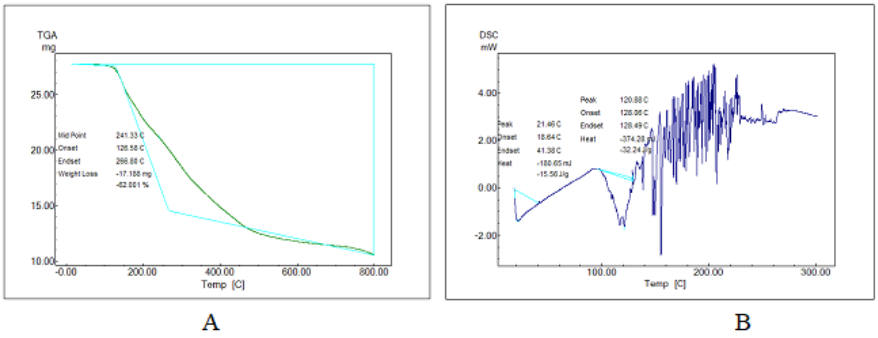

A B

Figure 4

TGA and DSC analysis of *Tephrosia purpurea* extract

(A) Thermo gravimetric scan of *Tephrosia purpurea*

(B) Differential scanning colorimetry scan of *Tephrosia purpurea*

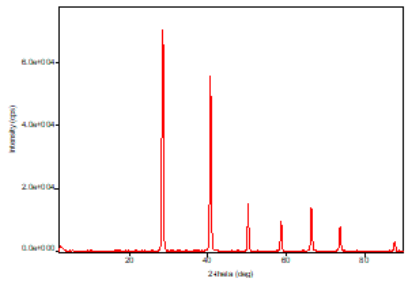

Figure 5

XRD patterns of the crystal structure of *Tephrosia purpurea* hydroethanolic extract

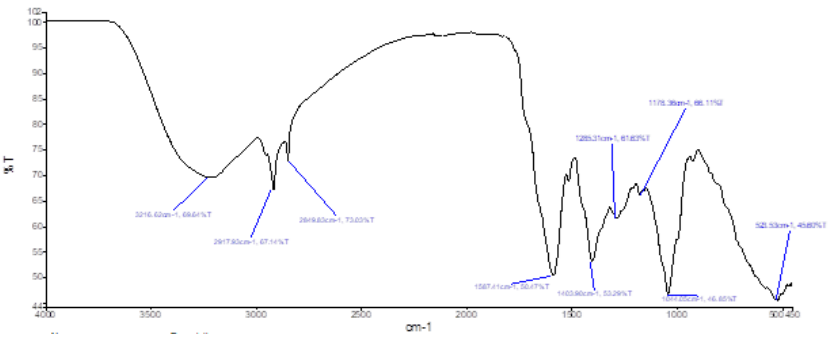

Figure 6

FTIR spectra of hydroethanolic extract of *Tephrosia purpurea*

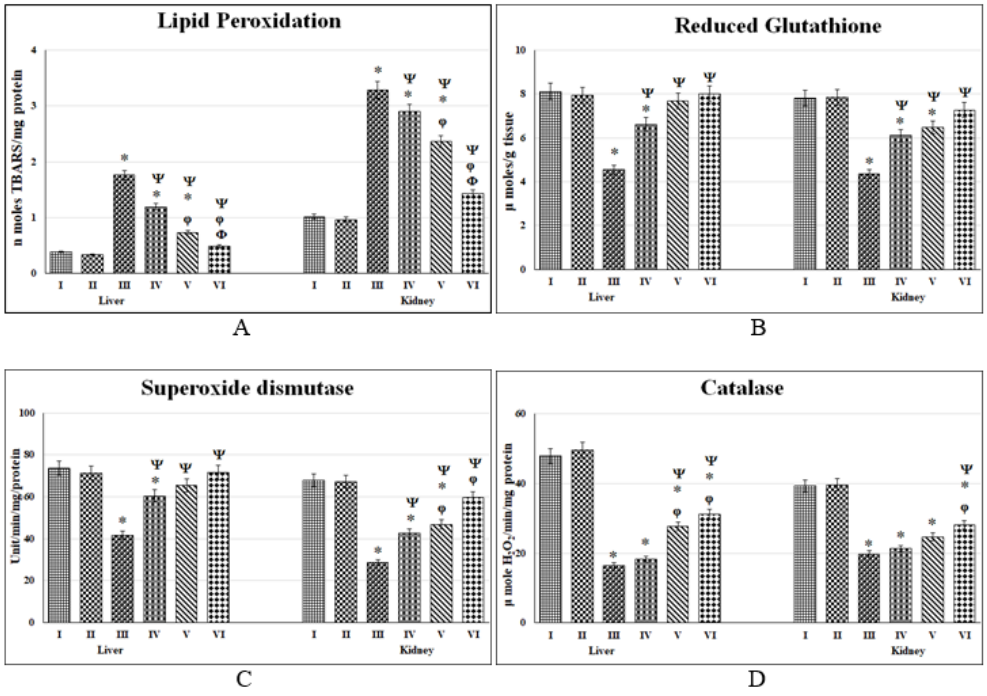

Figure 7

Protective efficacy of *Tephrosia purpurea* on lipid peroxidation, reduced glutathione, superoxide dismutase and catalase activity on hepatic and renal tissue against D-GalN and LPS induced oxidative stress

Data are expressed as mean ± SE, (n=6). *P≤0.05 versus Control. ʏP≤0.05 versus D-GalN+LPS. ʲP≤0.05 versus TP 50 mg/kg. ᶠP≤0.05 versus TP 100 mg/kg. I=Control group. II= TP 200 mg/kg group. III= D-GalN+LPS group. IV= D-GalN+LPS+ TP 50 mg/kg group. V= D-GalN+LPS + TP 100 mg/kg group. VI= D-GalN+LPS + TP 200 mg/kg group.

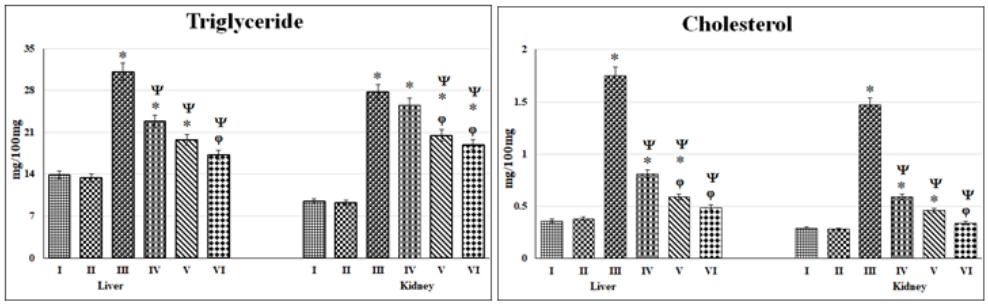

Figure 8

Protective potential of *Tephrosia purpurea* against D-GalN and LPS induced changes in hepatorenal triglyceride and cholesterol contents

Data are expressed as mean ± SE, (n=6). *P≤0.05 versus Control. ʏP≤0.05 versus D-GalN+LPS. ʲP≤0.05 versus TP 50 mg/kg. ꜰP≤0.05 versus TP 100 mg/kg. I=Control group. II= TP 200 mg/kg group. III= D-GalN+LPS group. IV= D-GalN+LPS+ TP 50 mg/kg group. V= D-GalN+LPS + TP 100 mg/kg group. VI= D-GalN+LPS + TP 200 mg/kg group.

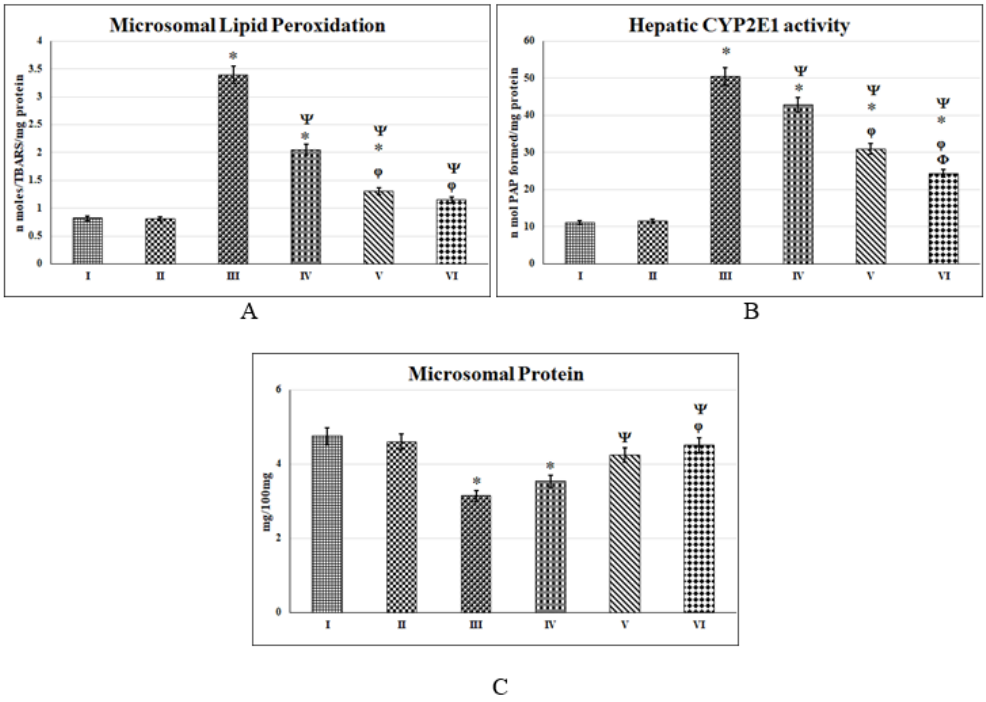

Figure 9

Protective efficacy of *Tephrosia purpurea* against D-GalN and LPS induced lipid peroxidation, CYP2E1 activity and protein on hepatic microsomes

Data are expressed as mean ± SE, (n=6). *P≤0.05 versus Control. ʏP≤0.05 versus D-GalN+LPS. ʲP≤0.05 versus TP 50 mg/kg. ꜰP≤0.05 versus TP 100 mg/kg. I=Control group. II= TP 200 mg/kg group. III= D-GalN+LPS group. IV= D-GalN+LPS+ TP 50 mg/kg group. V= D-GalN+LPS + TP 100 mg/kg group. VI= D-GalN+LPS + TP 200 mg/kg group.

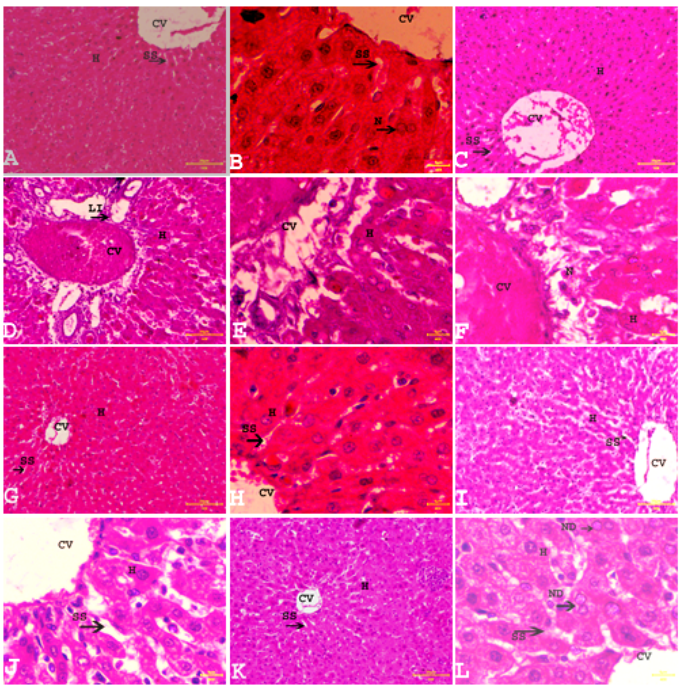

Figure 10

Histological observation of rat liver sections under light microscope

A: control (10X); B: control (40X); C: TP *per se* (10X); D: D-GalN+ LPS (10X); E and F: D-GalN+ LPS (40X); G: TP 50 (10X); H: TP 50 (40X); I: TP 100 (10X); J: TP 100 (40X); K: TP 200 (10X); L: TP 200 (40X); K: Kupffer cell; N: Nucleus; ND: Nuclear division; Figure A and B shows regular structure of liver with tightly packed pink stained hepatocytes. The sinusoidal space (SS) can be seen as pale stained spaces between the cord of hepatocytes. Micrograph C shows hepatic architecture with central vein (CV), array of hepatocytes (H) and sinusoidal space (SS). Photomicrograph D, E and F shows hepatic centrilobular mononuclear cell infiltration (LI), distortion in shape of central vein and dilation in sinusoidal spaces (SS). Figures G-H, I-J and K-L shows a gradual recovery pattern with increasing dose of *Tephrosia purpurea*. Well-shaped CV, surrounded by array of hepatocytes, proper sinusoidal spaces and lesser number of neutrophils were also observed.

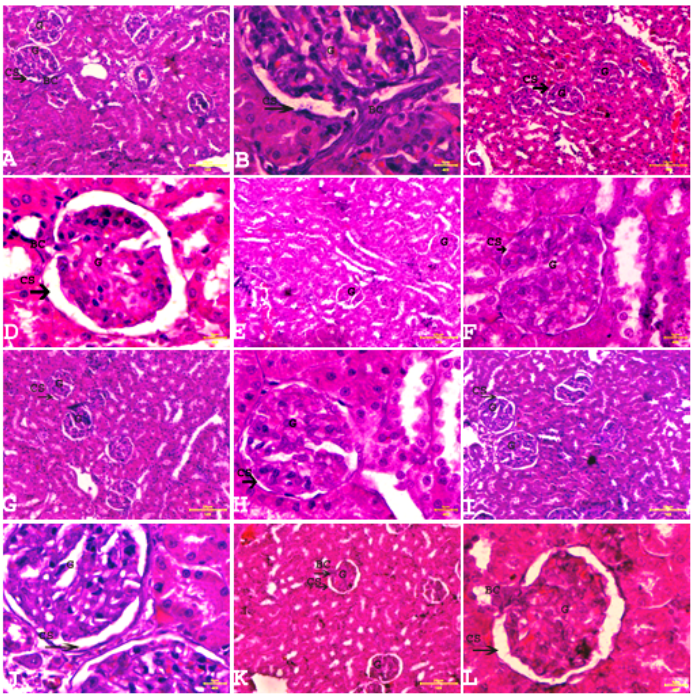

Figure 11

Histological observation of rat kidney sections under light microscope

A: control (10X); B: control (40X); C: TP *per se* (10X); D: TP *per se* (40X); E: D-GalN+ LPS (10X); F: D-GalN+ LPS (40X); G: TP 50 (10X); H: TP 50 (40X); I: TP 100 (10X); J: TP 100 (40X); K: TP 200 (10X); L: TP 200 (40X); BC: Bowman's capsule; CS: Capsular space; G: Glomerulus. Figure A-D shows peculiar histoarchitecture of kidney with normal glomerulus (G) and Bowman's capsule (BC). Figure E and F of kidney treated with LPS and D-GalN indicated swelling in glomerulus that occupied maximum capsular space of Bowman's capsule and disturbed cellular matrix of Bowman's capsule. Representation of figure G-H, I-J, and K-L of kidney shows gradual recovery pattern increasing dose of *Tephrosia* purpurea as evident by well-shaped glomerulus with reduced swelling and more capsular spaces (CS). The cellular matrix of Bowman's capsule of purpurin treated groups is similar to histological appearance of control group.

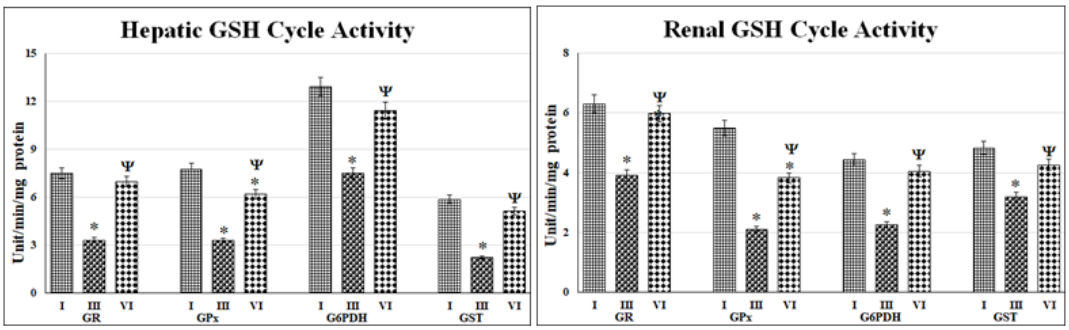

Figure 12

Protective potential of *Tephrosia purpurea* on D-GalN and LPS induced alteration in hepatorenal GSH cycle

Data are expressed as mean ± SE, (n=6). *P≤0.05 versus Control. ʏP≤0.05 versus D-GalN+LPS. ᴊP≤0.05 versus TP 50 mg/kg. FP≤0.05 versus TP 100 mg/kg. I=Control group. III= D-GalN+LPS group. VI= D-GalN+LPS + TP 200 mg/kg group.

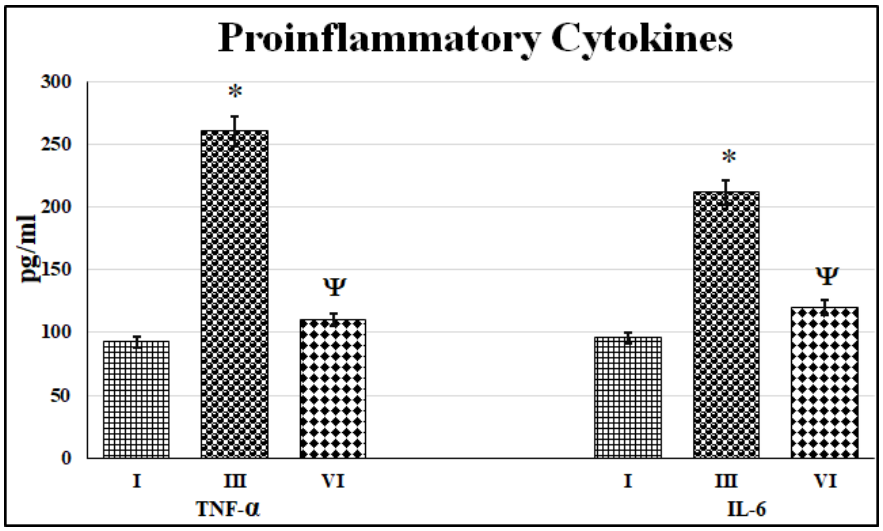

Figure 13

Protective potential of *Tephrosia purpurea* on D-GalN and LPS induced alteration in serum TNF-α and IL-6

Data are expressed as mean ± SE, (n=6). *P≤0.05 versus Control. ʏP≤0.05 versus D-GalN+LPS. ᴊP≤0.05 versus TP 50 mg/kg. FP≤0.05 versus TP 100 mg/kg. I=Control group. III= D-GalN+LPS group. VI= D-GalN+LPS + TP 200 mg/kg group.

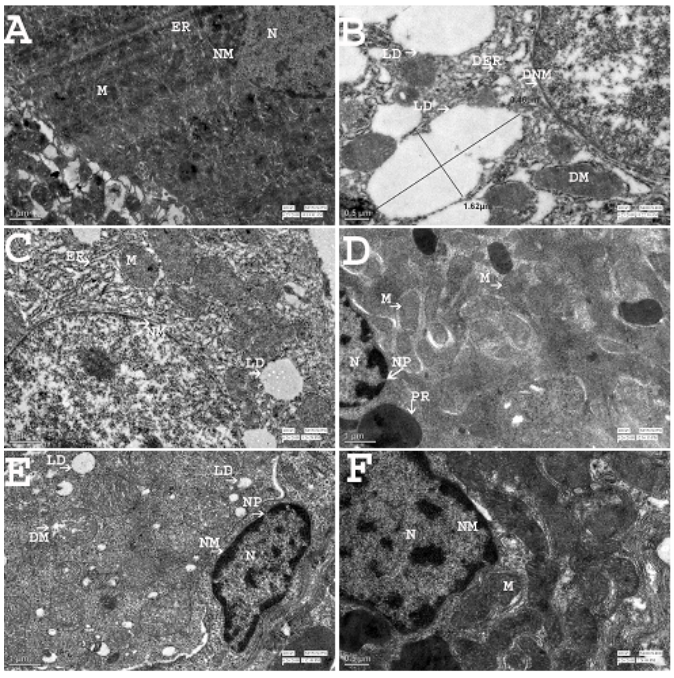

Figure 14

Ultrastructural observation of rat liver and kidney under transmission electron microscope

Figure 14A (2550X) represents electron micrograph of liver of control group, figure 14B (2550X) represents liver of D-GalN and LPS exposed group and figure 14C (2550X) represents liver of prophylactic treatment with *Tephrosia purpurea* at 200 mg/kg dose followed by D-GalN and LPS.

Electron micrograph of kidney of control group treated with vehicle only is shown in figure 14D (2550X), figure 14B (2550X) represents kidney of D-GalN and LPS exposed group and figure 14C (2550X) represents kidney of prophylactic treatment with *Tephrosia purpurea* at 200 mg/kg dose followed by D-GalN and LPS.

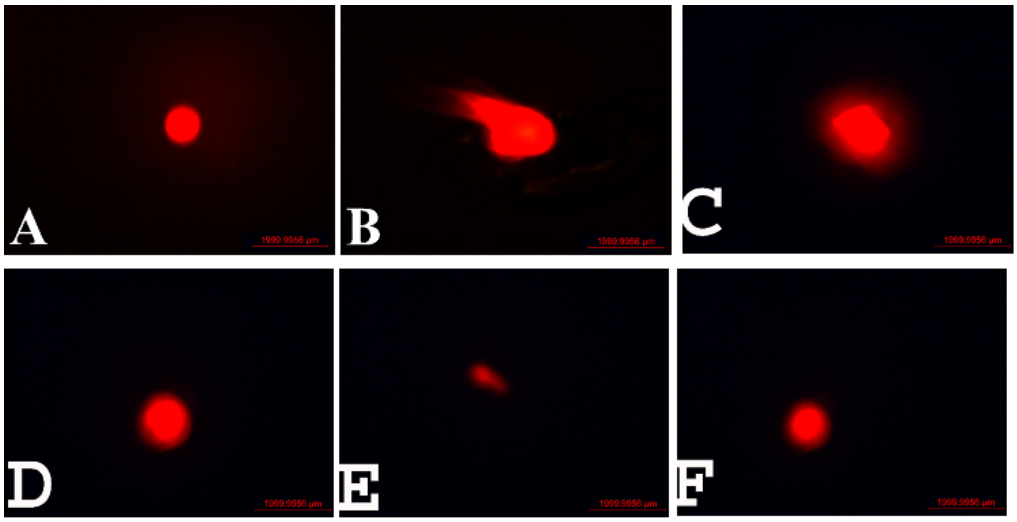

Figure 15

Protective efficacy of *Tephrosia purpurea* on D-GalN and LPS induced genotoxicity

Photographs of liver section obtained from comet assay analysis were presented from A to C, while kidney sections were presented from D to F. A and D: control; B and E: D-GalN + LPS only; C and F: TP 200 with D-GalN + LPS. Photomicrographs of control group shows round shaped nucleus with compact DNA. The D-GalN + LPS treated group shows formation of a comet shaped appearance of nuclear material in liver (B) and kidney (E) indicating DNA damage. Animals treated with *Tephrosia purpurea* at 200 mg/kg dose showed lesser head and tail (comet) of nuclear material in liver (C) and kidney (F) as a sign of protection of DNA.